SU-SEL-66-021

High-Frequency Measurement of Radar Cross Section Using the Standing-Wave Method

by

J. G. Steele and J. R. Barnum

March 1966

Technical Report No. 127

Prepared under
Office of Naval Research Contract
Nonr-225(64), NR 088 019, and
Advanced Research Projects Agency ARPA Order 196-65

RADIOSCIENCE LABORATORY

STANFORD ELECTRONICS LABORATORIES

STANFORD UNIVERSITY · STANFORD, CALIFORNIA

DISCLAIMER NOTICE

THIS DOCUMENT IS BEST QUALITY PRACTICABLE. THE COPY FURNISHED TO DTIC CONTAINED A SIGNIFICANT NUMBER OF PAGES WHICH DO NOT REPRODUCE LEGIBLY.

SEL-66-021

HIGH-FREQUENCY MEASUREMENT OF RADAR CROSS SECTION USING THE STANDING-WAVE METHOD

by

J. G. Steele and J. R. Barnum

March 1966

Technical Report No. 127
Prepared under
Office of Naval Research Contract
Nonr-225(64), NR 088 019, and
Advanced Research Projects Agency ARPA Order 196-65

Radioscience Laboratory
Stanford Electronics Laboratories
Stanford University Stanford, California

ABSTRACT

The standing-wave method of measuring radar cross sections has been adapted for use at 26 Mc. A target in the middle of a large flat field was illuminated by a transmitter 300 feet away, and a probe was moved along the transmitter-target line to measure the amplitude and position of the standing wave due to the target.

Aluminum dipoles of different lengths were first used as targets, and a correction was applied to the results to take account of any non-uniform illumination of the targets. Both the target cross section and the phase of the scattered radiation varied with the target length in the same way as that predicted from microwave measurements. The results demonstrate the validity of extrapolating microwave measurements to the high-frequency part of the spectrum. Calibration of the system was achieved by using the known cross section of a half-wave dipole.

The technique was used to measure cross sections of trees and other objects, and in some cases the "effective height" of an irregularly shaped tree could be deduced.

CONTENTS

TABLES

ILLUSTRATIONS

SYMBOLS

a	radius of cylinder
b	a measure of the reflected amplitude
B	relative cross section when $I = 1$
E_i	amplitude of the unperturbed field at the range of the target and at a standard height
E_s	amplitude of the scattered field at a given range from the target
f	radio frequency
G	relative gain of transmitting antenna
h	height above ground, or half-length of dipole
I	illumination factor
I_h	illumination factor for a horizontal cylinder at height h
I_L	illumination factor for a vertical cylinder of length L
J	a measure of the relative gain of transmitting antenna
k	$2\pi/\lambda$
L	length of cylinder
r	range
V	voltage reading at 25.9-Mc transmitter
w	range from target in direction of transmitter
w_1	displacement of standing wave from the position it assumes when the first minimum is at $w = 0$
θ	deflection of axis of cylinder
λ	wavelength = 38 ft
σ	radar cross section
ϕ	amount by which the phase change on reflection is less than π radians

ACKNOWLEDGMENT

The authors wish [illegible] r., Director of the Radioscience Labo[illegible] encouragement. The cooperation of [illegible] ence Laboratory is much appreciated. Mr. J[illegible] [illegible]meron assisted in the collection and reduct[illegible] [illegible] Weedon assisted in the construction of the pr[illegible]

The Ov[illegible] [illegible]uate Studentship awarded to J. G. Steele by the Commonwealth Scientific and Industrial Research Organization (CSIRO) of Australia is gratefully acknowledged, as is the hospitality of Stanford University during the tenure of that studentship.

I. INTRODUCTION

In the high-frequency range (3 to 30 Mc), radar cross sections are of interest in connection with ground backscatter and with oblique sounding of the ionosphere by means of ground backscatter. The backscatter coefficient, or radar cross section per unit area of the ground, is a measure of the strength of a backscatter echo from a given type of terrain and at a given angle of incidence.

It has been suggested [Refs. 1, 2] that the energy scattered back from land surfaces is largely due to scattering from upright targets such as trees, and that interference between direct and ground-reflected rays discriminates against low-angle radiation reaching or leaving the target.

This report describes the measurement of the free-space cross sections of trees and other objects. Although these targets were on or near the ground, data reduction was performed in such a way that ground effects were eliminated from the results. In a subsequent report it is hoped to present cross sections of "objects on the ground" (that is, the ground will be considered as part of the target) as in ground backscatter.

For the free-space cross sections dealt with here, it is of interest to know if a given tree scatters like a conducting dipole, with a definite target length and resonant frequencies, and also whether high-frequency results for conducting dipoles are comparable to microwave results for such targets.

Microwave results for conducting dipoles were obtained by King [Ref. 3], Sevick [Ref. 4], and Å and Schmitt [Ref. 5] and their results agree quite well with the approximate theoretical results of Van Vleck et al [Ref. 6] and Lindroth [Ref. 7], as discussed by King and Wu [Ref. 8]. In all these investigations it was found that if σ is the radar cross section of the dipole when the electric field is parallel to its axis and λ is the wavelength, σ/λ^2 passes through resonance maxima for dipole lengths of $\lambda/2$, $3\lambda/2$, etc. Also, σ/λ^2 has a value of 0.88 for a half-wave dipole, which suggests a means of calibrating the high-frequency measurements.

II. METHOD

The method used here for measuring cross sections is an adaptation of the standing-wave method described in Refs. 3 and 8. In the standing-wave method, a receiving probe is moved along a straight line between the transmitter and the target, and the field strength is recorded as a function of position. This field is the vector sum of the direct and scattered fields, yielding a standing wave. Both direct and scattered components vary with range, and if their range dependence is known, the target cross section can be calculated from the data.

In microwave work, the standing-wave method was developed for use where the transmitting antenna, target, and probe could be placed on a highly conducting image plane. This plane served to screen all auxiliary equipment and connecting cables from the region of measurement and to insure that the amplitudes of the two fields each decreased with range r as $1/r$.

At high frequency an image plane cannot be constructed, owing to the much larger distances involved. Wavelengths range from 10 to 100 meters; targets of interest are about half a wavelength or larger in size, and it is desirable for the transmitting antenna to be about this size as well. To achieve any kind of approximation to plane-wave illumination of the target, the spacing between the transmitter and the target must be about 5λ. Perhaps salt water could be used as an image plane, but the targets proposed in the present work do not allow such treatment.

Two problems arise from the lack of a good image plane. The first is that connecting cables must be eliminated or reduced to a minimum and that people and equipment in the vicinity of the target or probe must be considered as part of the target or probe. To eliminate a cable from the probe to the control room, the probe was constructed with its own detector, voltage comparator, and telemeter. Readings were taken by varying the transmitter output until the telemeter registered comparator equality and then noting the transmitter output V. The field at the probe for a constant transmitter output is then proportional

to the reciprocal of the reading taken. A man moving in the vicinity of the probe can be thought of as a parasitic element. The signal received was found to vary with the man's movements and he therefore was assigned a standard position relative to the probe--15 ft from the probe toward the transmitter--where his position was not critical.

The second disadvantage of not having a good image plane is that one has instead the natural earth, which conducts poorly. The range dependence is no longer $1/r$, but varies, approaching $1/r^2$. This variation makes the direct calculation of cross sections very difficult. Also, a target with vertical extent is not uniformly illuminated by the transmitter. Again, more power is required to illuminate the target sufficiently. Further, the scattered field diminishes rapidly with range from the target, and if the cross section is small, the probe must be moved very close to the target to detect the scattered field, and thus can no longer be said to receive plane waves from the target. Methods have, however, been devised to handle these problems, and good results have been obtained even for horizontal polarization, which is not possible with the simple image-plane technique. Further, one of the problems associated with the use of an image plane, namely the residual standing waves due to reflections from the ends of the conducting screen, does not arise.

Figure 1 is a schematic diagram of the standing-wave method as developed here. The frequency used was 25.9 Mc (λ = 38 ft); although this value is at the higher end of the high-frequency range, this choice was necessary to avoid building quite enormous antennas so far from the target that the available site would have been inadequate. In any case,

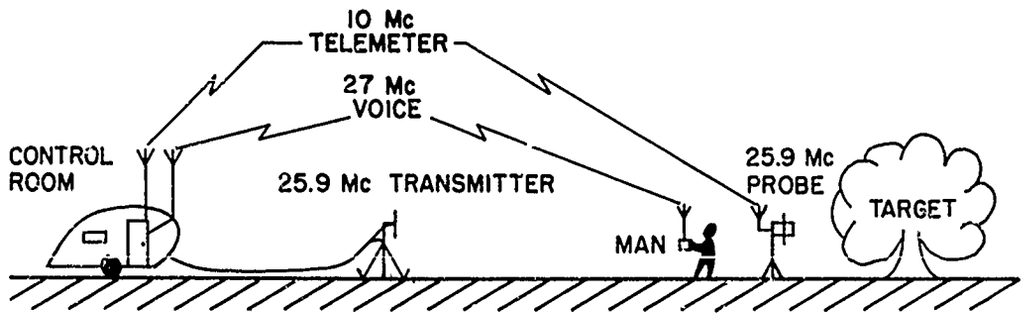

FIG. 1. SCHEMATIC DIAGRAM OF THE STANDING-WAVE METHOD.

it will be seen that the results of the project justify their extrapolation to other parts of the high-frequency range. With the transmitter 300 ft from the target, plane-wave illumination was assumed for targets up to 30 ft long.

The probe was normally 20 to 60 ft from the target and so did not receive plane waves from the target. Because of this, the measured cross section of a 30-ft target was perhaps 10 percent too small [Ref. 8, p. 135].

Figure 2 is an aerial photograph of the site on which the measurements were carried out. It was a level, ploughed field, free of trees except for several isolated oak trees serving as targets. In the figure, T is the transmitter; I, II, and III are the trees discussed in Chapter VI; and L is the street light discussed in Chapter VII.

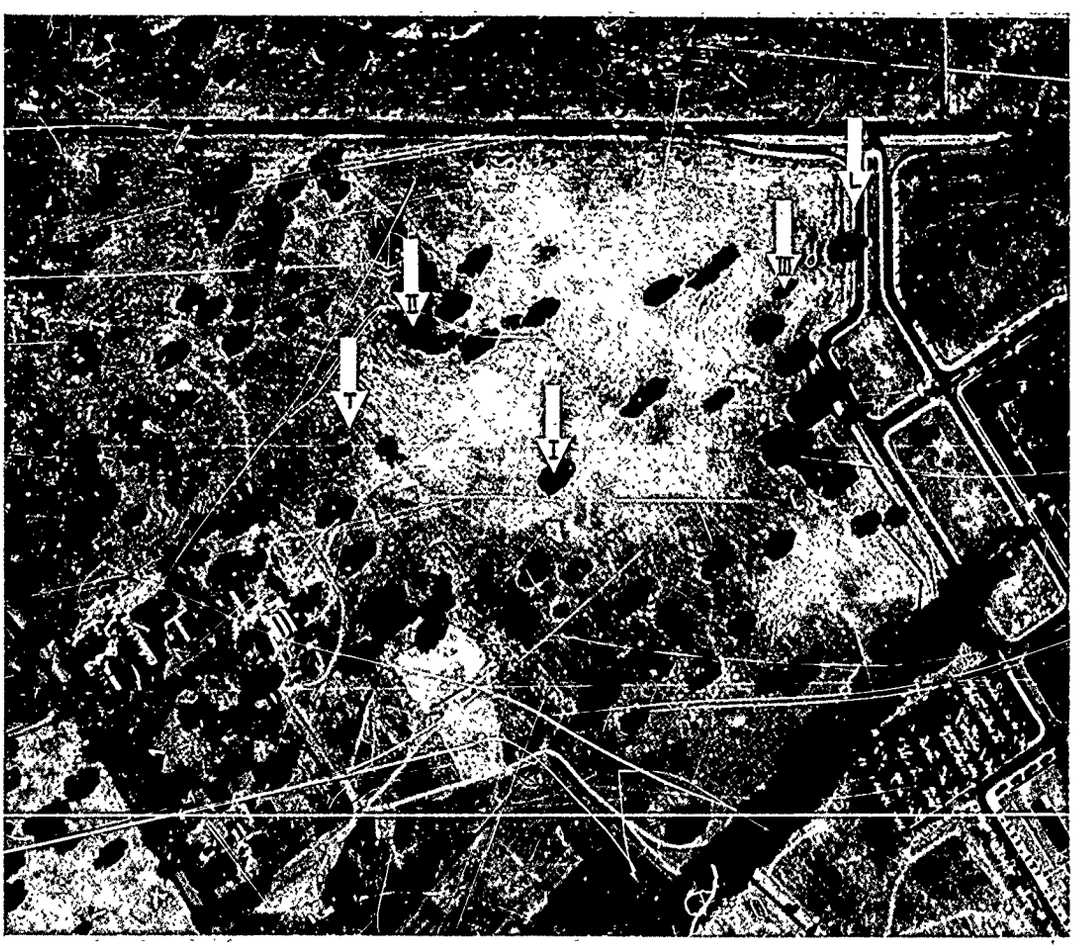

FIG. 2. AERIAL PHOTOGRAPH OF TEST SITE SHOWING LOCATIONS OF TARGETS.

Figure 3 is a block diagram showing the equipment used; this equipment is listed in Table 1. The probe and associated telemeter will be described in detail in Chapter III. The 25.9-Mc transmitter was capable of delivering 350 w of cw power to a coaxial line, and the voltmeter from which readings were taken was applied at this point. Near the transmitting antenna, the coaxial line was shielded every few feet with ferrite cylinders. The transmitting antenna was a center-fed, half-wave loaded dipole, 10 ft long, mounted with its center 10 ft above the ground. The probe antenna was a center-fed loaded dipole, 5 ft 3 in. long, with its center 8 ft above ground, and its polarization was always parallel to that of the transmitting antenna.

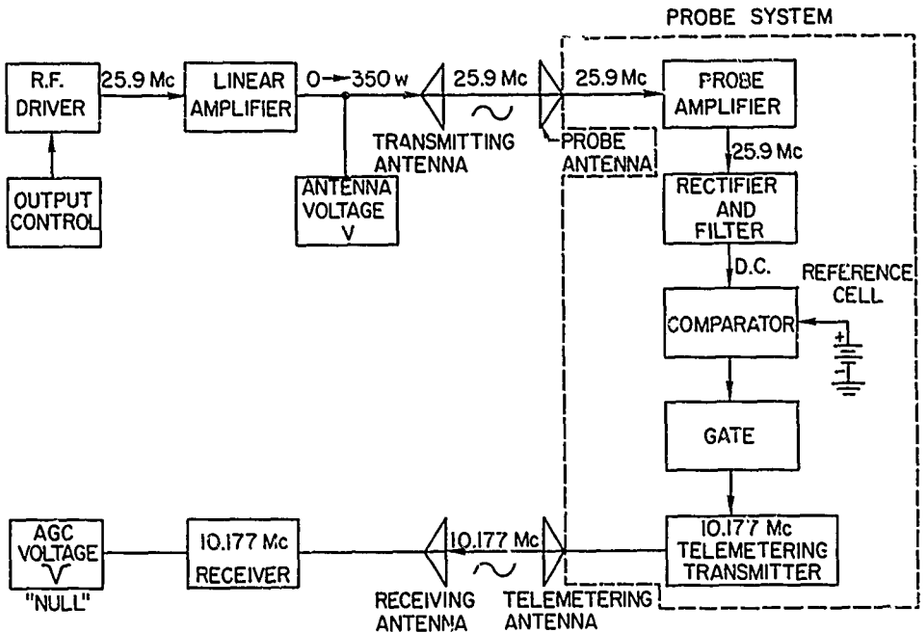

FIG. 3. BLOCK DIAGRAM OF EQUIPMENT USED FOR MEASURING CROSS SECTIONS.

The telemeter operated at 10.177 Mc, and when a balance was achieved in the voltage comparator, the 10.177-Mc signal dropped to a sharp minimum, which was observed on the second voltmeter in the control room.

The data obtained for a given target varied according to the nature of the target. Typically, in order to obtain the standing waves the "perturbed field" was measured by taking readings every 2.5 ft up

TABLE 1. EQUIPMENT USED IN MEASURING CROSS SECTIONS

RF driver	Collins 32S-1
Linear amplifier	Collins 30S-1
Voltmeters	Hewlett-Packard hp-410-B
Receiver	Collins 75S-1
Transmitting antenna	Half-wavelength resonant loaded dipole
Probe antenna	Short doublet
Telemetering antenna	4-ft wire fastened vertically to the probe stand
Receiving antenna	Long wire
Probe system	See Chapter III

to 50 ft from the target. If the target was removable, the "unperturbed field" was measured at intervals of 10 ft. A set of data for a given target could usually be obtained in 15 min.

Figure 4 shows some of the data obtained. The axes of the graph are graduated in reverse because, by convention, here the direction of the incident radiation is from left to right and because a smaller voltage reading indicates a larger "field per given transmitter output." The voltage values are much larger for horizontal polarization than for vertical, as the ground effect caused more distance attenuation and required more transmitted power to activate the telemeter. However, in both cases the amplitude of the standing wave was a significant fraction of the total field reaching the probe.

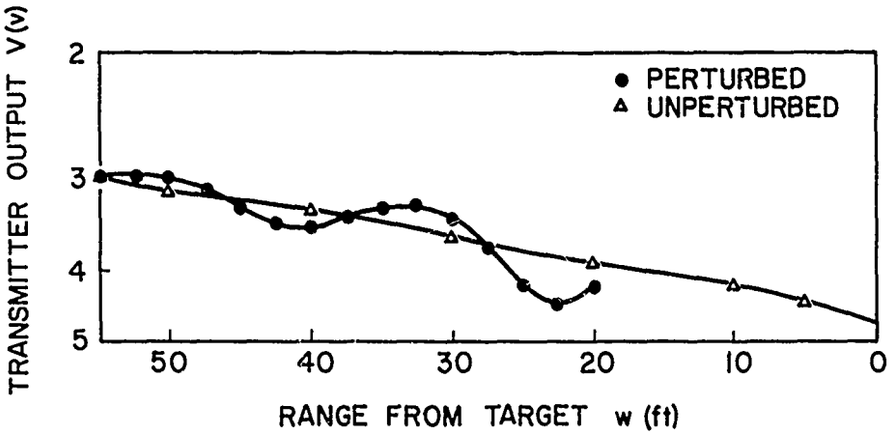

a. Vertical polarization, 8-ft vertical grounded cylinder

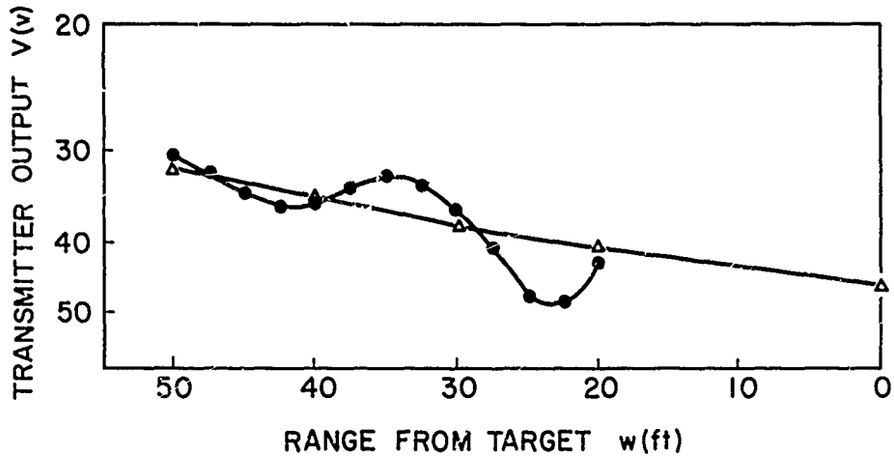

b. Horizontal polarization, 17-ft horizontal cylinder 8 ft above the ground

FIG. 4. DATA FOR ALUMINUM CYLINDERS.

III. CONSTRUCTION AND PERFORMANCE OF THE PROBE AND TELEMETER

A photograph of the probe, with one side removed to show the interior construction, is given in Fig. 5. The 25 9-Mc amplifier, rectifier, and filter were mounted in a closed box for shielding purposes, while the 10.177-Mc telemetering transmitter, voltage comparator, and gate were mounted on cards. There was no perceptible interaction between the 25.9-Mc and the 10.177-Mc systems.

Mercury batteries were used throughout to insure constant voltage. External controls were provided to tune the 25.9-Mc amplifier and the 10.177-Mc transmitter, and to switch the batteries in and out of the circuit.

The probe antenna, partly shown in Fig. 5, was insulated from the chassis and was matched to the amplifier by means of an external coil. The telemetering antenna (not shown) was a 4-ft length of wire attached to the probe stand and plugged into the probe when required. This stand was a wooden pole 8 ft high, and the probe could be bolted to the top of it in either the vertical or horizontal positions. When in the vertical position, the probe antenna was parallel to, and a few inches from, the telemetering antenna, but the effect was only a slight constant amplification of the field being measured. Most important, however, was the fact that both the probe antenna and the telemetering antenna were short enough to have a negligible effect on the fields being measured; this is confirmed by the measurements of cross sections of aluminum dipoles in Chapter V, which show that dipoles shorter than 10 ft have cross sections at 25.9 Mc too small to be measured by the present system.

The circuitry for the 25.9-Mc probe amplifier, rectifier and filter is shown in Fig. 6, and the applicable parts list is given in Table 2. The input impedance was about 50 ohms. The 3-db bandwidth was about 180 kc, and the available power gain was 80 db. Temperature stability was achieved through the use of the thermistor. In the warmer months of the year, temperature drift in the readings was negligible, owing to proper adjustment of the thermistor compensation network. In the colder months, it was found necessary to readjust the thermistor network; even so, a slight monotonic drift occurred, but the drift did not appreciably

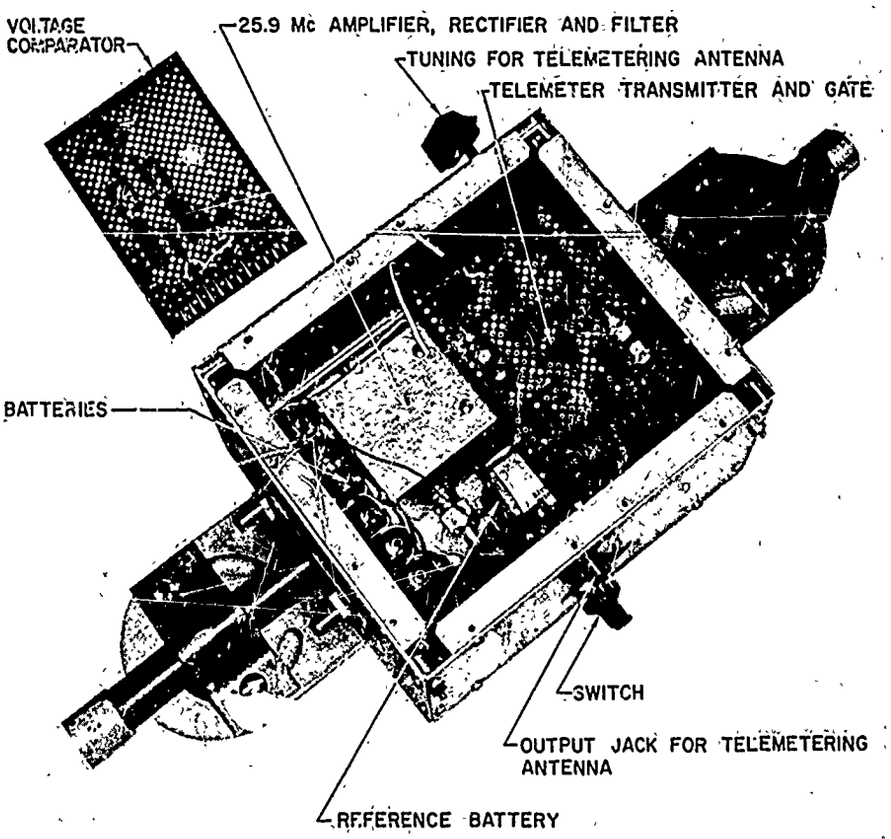

FIG. 5. PROBE DISMANTLED TO SHOW CONSTRUCTION.

hamper the successful reduction of the data, provided a set of data, for a given target, was taken within, say, 30 min.

The circuit diagram for the telemetering transmitter, voltage comparator, and gate is shown in Fig. 7, and the parts list is given in Table 3. The performance of this system may be seen in Fig. 8, which is a graph of the relative output of the telemetering transmitter vs normalized antenna voltage of the 25.9-Mc transmitter. Since the null could always be found below -16 db, the error in the voltage reading should be less than about ±0.04 db. However, at times the noise level due to other transmitters was high, causing a broadening of the null.

The errors in measuring voltages with the probe will now be considered. Errors may be due to misalignment and misplacement of the probe, faulty calibration and misreading of the meter, null broadening due to noise, and temperature drift in the probe amplifier.

An error analysis was performed on three separate sets of 27 readings taken on the near side of an oak tree (designated Tree I in Chapter VI). Each set was taken at intervals of 2.5 ft between 35 and 100 ft from the trunk. At 35 ft, the three readings were identical, suggesting that the errors, if any, will be small.

According to custom (see Chapter IV), the voltage readings V were inverted. Then, at each position of measurement, the three values of $1/V$ were averaged and the three "percentage deviations from the mean" were calculated. The distribution of the errors was plotted in Fig. 9. Of the 81 readings, 76 (or 94 percent) had a deviation less than 1.1 percent, which is less than 0.1 db.

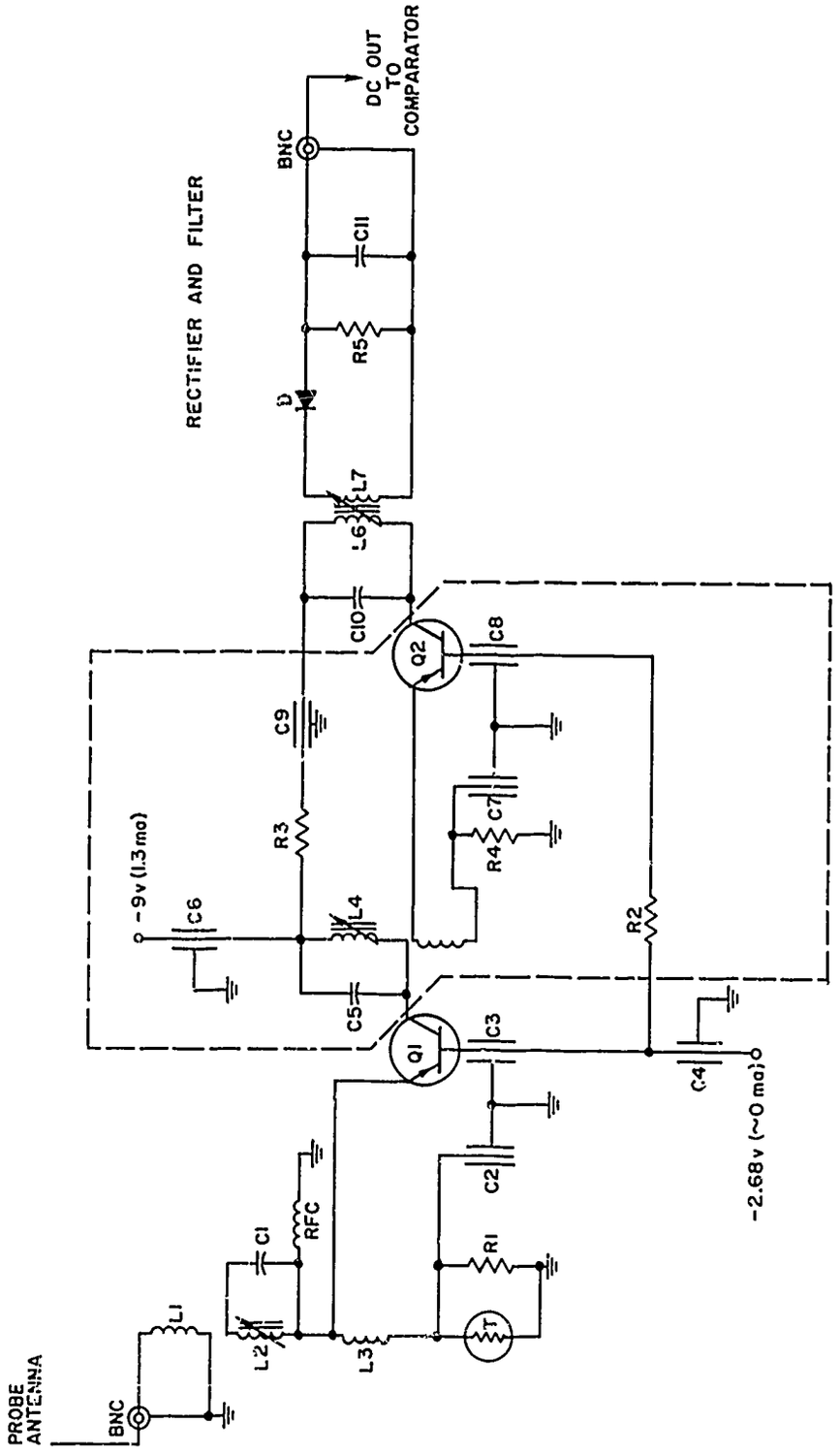

FIG. 6. CIRCUIT DIAGRAM FOR 25.9-Mc PROBE AMPLIFIER, RECTIFIER, AND FILTER.

TABLE 2. PARTS LIST FOR PROBE AMPLIFIER, RECTIFIER, AND FILTER

R1 = 2.2 kΩ

R2, R3 = 47 Ω

R4 = 1 kΩ

R5 = 47 kΩ

C1, C10 = 100 pf

C2, C3, C4, C6, C7, C8, C9 = 1500 pf feedthrough

C5 = 75 pf

C11 = 910 pf

L1 = 3/4 turns
L2, L4, L6, L7 = 7 turns
L3, L5 = 5/4 turns
} 3/16 dia., slug tuned

RFC = 100 μh

T1, T2 = 2N3640

D = 1N7714

J1, J2 = BNC

T = thermistor, 400 Ω $\leq R_T \leq$ 4.5 kΩ

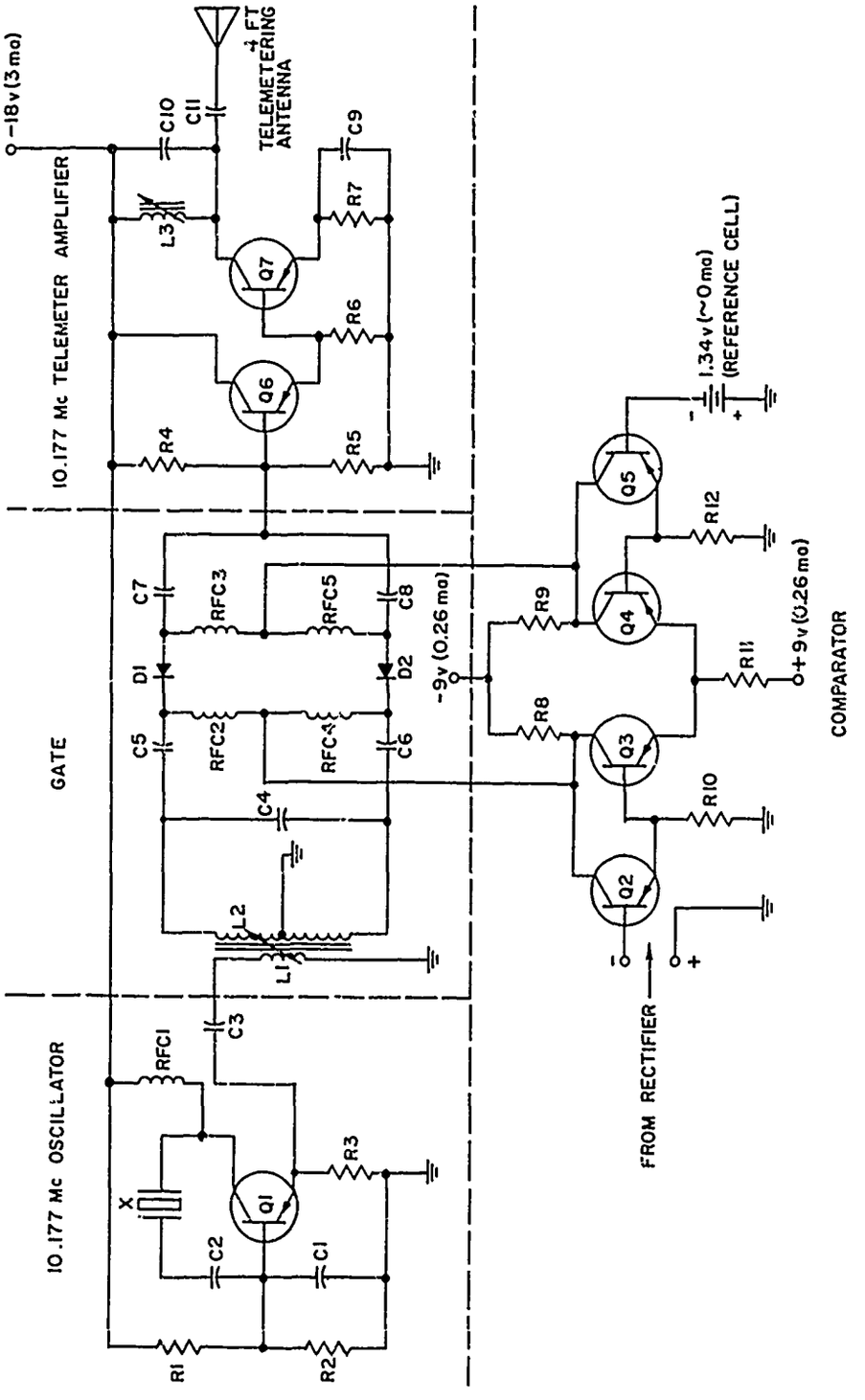

FIG. 7. CIRCUIT DIAGRAM FOR TELEMETERING TRANSMITTER, COMPARATOR, AND GATE.

TABLE 3. PARTS LIST FOR TELEMETERING TRANSMITTER, VOLTAGE COMPARATOR, AND GATE

R1, R2, R4, R5 = 47 kΩ

R3 = 5.6 kΩ

R6 = 12 kΩ

R7 = 3.9 kΩ

R8, R9, R11 = 33 kΩ

R10, R12 = 10 kΩ

C1 = 47 pf mica

C2, C3, C5, C6, C7, C8, C9, C11 = 0.02 μf mica

C4 = 75 pf mica

C10 = 68 pf mica

RFC1, RFC2, RFC3, RFC4, RFC5 = 1 mh

L1 = 5 turns 3/16 in. dia. wound between L2, slug tuned

L2 = 6 turns 3/8 in. spacing, 6 turns center tapped, slug tuned

L3 = 3 - 5 μh, slug tuned

T1, T6, T7 = 2N3640

T2, T3, T4, T5 = 2N3638 β-matched

D1, D2 = 1N696 resistance matched

X = 10.177 Mc crystal

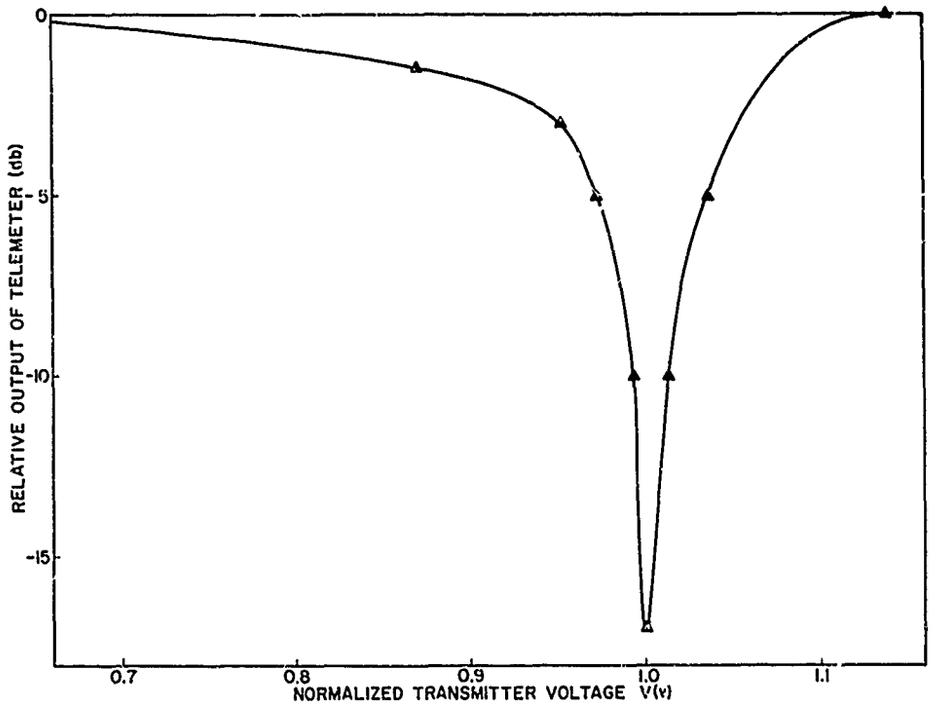

FIG. 8. TELEMETER OUTPUT VS 25.9-Mc TRANSMITTER VOLTAGE.

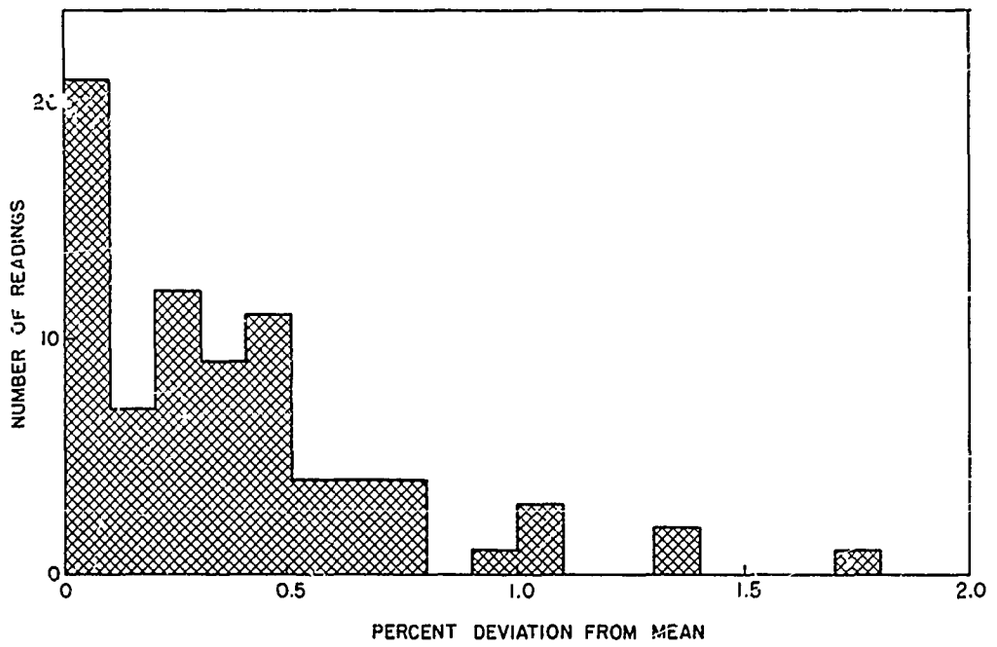

FIG. 9. PERCENTAGE DEVIATION FROM THE MEAN FOR THREE SETS OF 27 READINGS OF TRANSMITTER VOLTAGE.

IV. DATA REDUCTION

The cross section σ of a target may be obtained by reducing the data for that target in the following manner. The first stage is to plot the reciprocals $1/V$ of the measured voltages. For example, the data shown in Fig. 4 transforms to give the relative field strength at the probe in the presence and absence of the respective targets for constant transmitter output, which is illustrated in Figs. 10a and 10b.

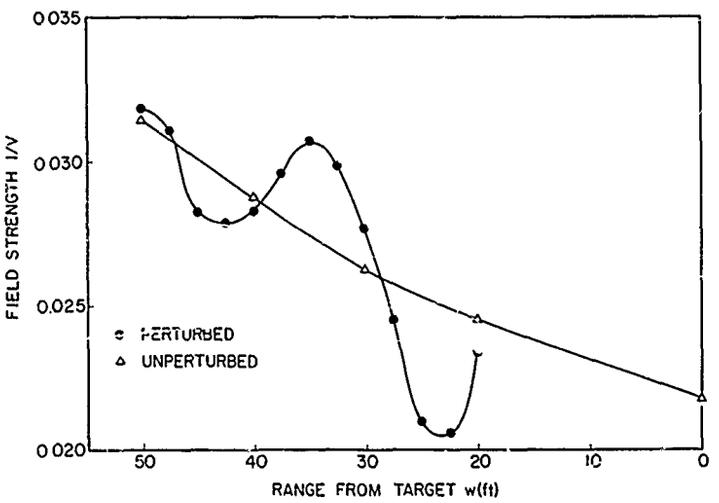

a. Horizontal polarization, 17-ft cylinder

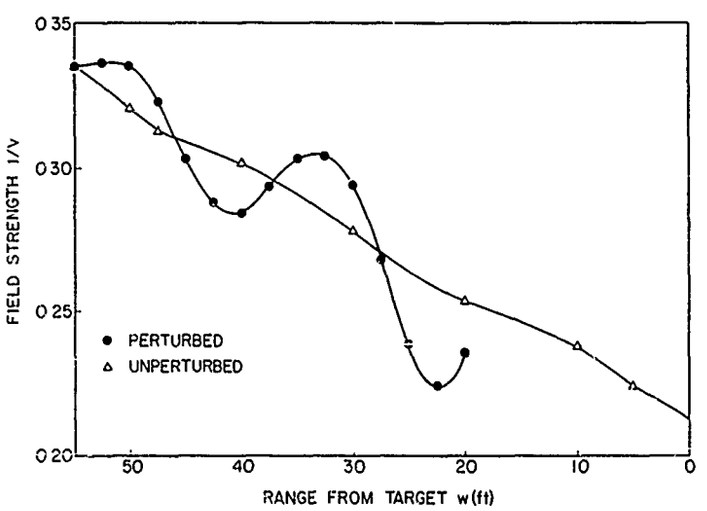

b. Vertical polarization, 8-ft cylinder

FIG. 10. FIELD STRENGTH AT PROBE FOR CONSTANT TRANSMITTER OUTPUT.

If the range dependence of the direct and scattered components were a simple analytical function such as $1/r$, the cross section could be calculated directly from the amplitudes and ranges of the standing-wave maxima and minima [Ref. 3]. But, as this is not practicable here, a graphical method was devised to yield relative cross sections and these results were then calibrated from targets of known cross section.

The direct or "unperturbed" field was subtracted from the "perturbed" field to give a standing wave with maxima and minima of amplitude E_s. If the target was not removable, the unperturbed field was estimated by bisecting the oscillations in the perturbed field. The scattered component was proportional to the amplitudes E_s at their respective ranges w from the target.

The assumption was made that the range dependence of the scattered field is always the same, whatever the target length. When horizontal dipoles are used as targets, this is a good assumption, since they are of small vertical extent and may be kept at the same height above the ground. By plotting $\log E_s$ vs $\log w$, it was possible to construct a standard curve which could be fitted to points plotted for horizontal dipoles of different cross sections.

Rather than plot E_s, it was found convenient to work in terms of the relative amplitude E_s/E_i. The field E_i, which is a measure of the illumination of the target, is the amplitude of the unperturbed field at the range of the target and at a standard height (usually 8 ft) above the ground.

Figure 11 is a graph of E_s/E_i vs w plotted on logarithmic paper, and the standard curve of range dependence is superimposed for the best fit to each set of data. Sometimes the points fell on alternate sides of the standard curve, because, in graphs of the type illustrated in Fig. 10, the curve for the unperturbed field did not exactly bisect the curve for the perturbed field. This failure was caused by a small change in the sensitivity of the probe between the times when the two sets of data were taken. Fitting the standard curve among the points of alternate positive and negative error was an effective way of canceling the error.

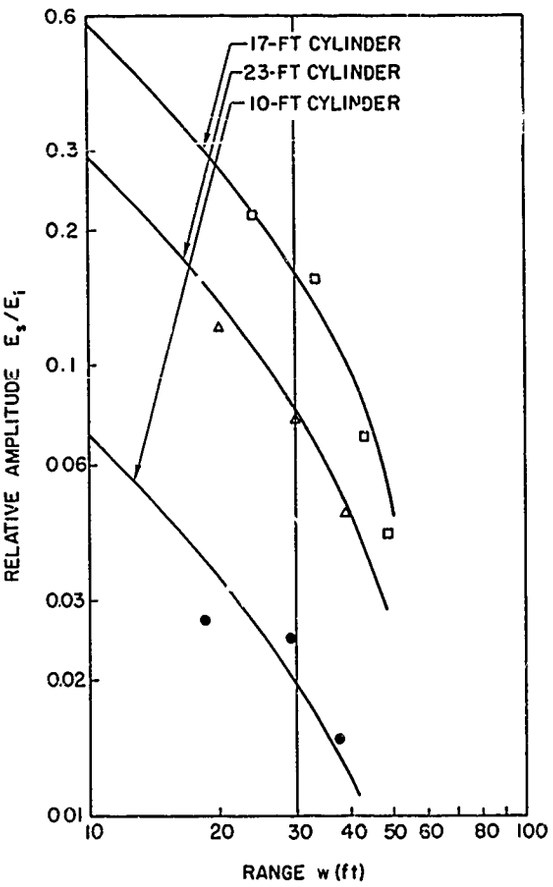

FIG. 11. RELATIVE AMPLITUDE OF BACKSCATTERED FIELD FOR HORIZONTAL CYLINDERS OF VARIOUS LENGTHS WITH THE STANDARD RANGE-DEPENDENCE CURVE SUPERIMPOSED.

For targets of different cross sections, the standard curve appears at different heights on Fig. 11. By convention, these heights were read off at w = 30 ft. This range is arbitrary but was chosen because both the data points and the standard curve were usually most accurate in this region.

The optimum range was a compromise between the need to be close enough to the target to detect the field perturbation due to the scattered

component, and the need to be far enough from the target to be able to assume plane waves.

The heights read from Fig. 11 were designated $(E_s/E_i)_{30}$, which on squaring became the relative cross section B. In some cases to be discussed later, the relative cross section is actually B/I, where I is an "illumination factor." The constant of proportionality relating B (or B/I) to σ can be determined, as shown in Chapter V, from a target of known cross section.

Comparing this treatment with the calculation of King [Ref. 3], we may liken $(E_s/E_i)_{30}$ to King's coefficient b, which he calls "a measure of the reflected amplitude." Then the cross section σ, given by King as $4\pi b^2$, is proportional to our relative cross section B.

So far, it has been assumed that the targets are horizontal dipoles of small vertical extent and at a constant height above the ground. If, however, the height above the ground is varied, there are two points to be considered: (1) the range dependence may vary for different target heights, and (2) the higher targets will receive more illumination per unit area, as they can take advantage of the larger gain of the transmitting antenna at higher angles of elevation.

This second point was investigated by moving the probe (horizontally polarized) up a wooden pole erected at the usual target position. If the relative power received (for constant transmitter output) is G_h at height h, we may define an illumination factor

$$I_h = G_h/G_8 ,$$

where G_8 is the same as E_i^2. This illumination factor may be used to modify E_i^2, so that the relative cross section is not B, but B/I_h. Figure 12 is a graph of I_h vs h for a target range of 300 ft.

For a vertical target standing on the ground, the target has vertical extent and its height above ground varies with its length. As with a horizontal target, its height will affect both the range dependence of the scattered field and the illumination of the target per unit area, but unlike the horizontal case, the illumination varies from one end of the target to the other.

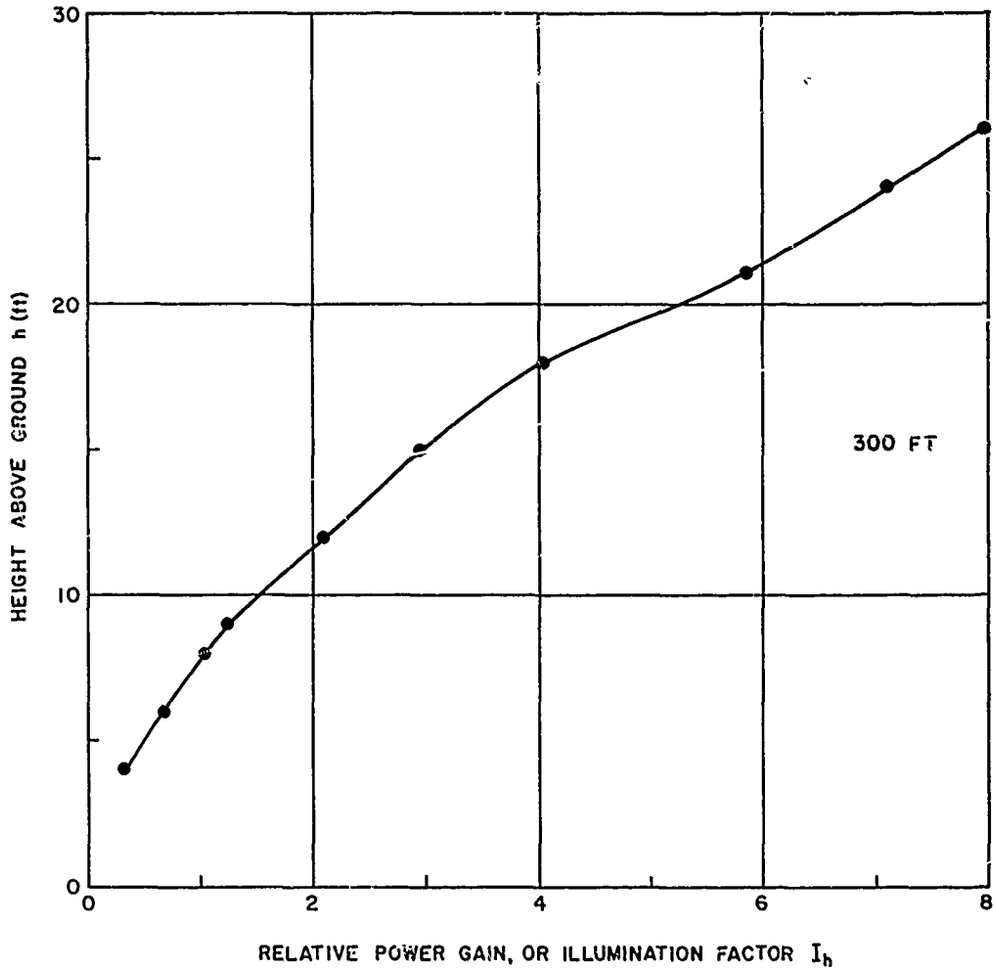

FIG. 12. RELATIVE POWER GAIN OF TRANSMITTING ANTENNA AT VARIOUS HEIGHTS ABOVE THE GROUND, FOR HORIZONTAL POLARIZATION.

Consider first the range dependence. Figure 13 repeats the procedure of Fig. 11, but this time for vertical targets and vertical polarization, and so the standard curve of range dependence is different from that of Fig. 11. The standard curve can be fitted fairly well to the plotted points, which suggests that the assumption of a standard curve is justified in these cases.

Secondly, for targets of vertical extent, the illumination per unit area of target increases with height. As for horizontal polarization, the relative power gain at height h was measured by moving the probe (now vertically polarized) up a wooden pole. But as the probe antenna

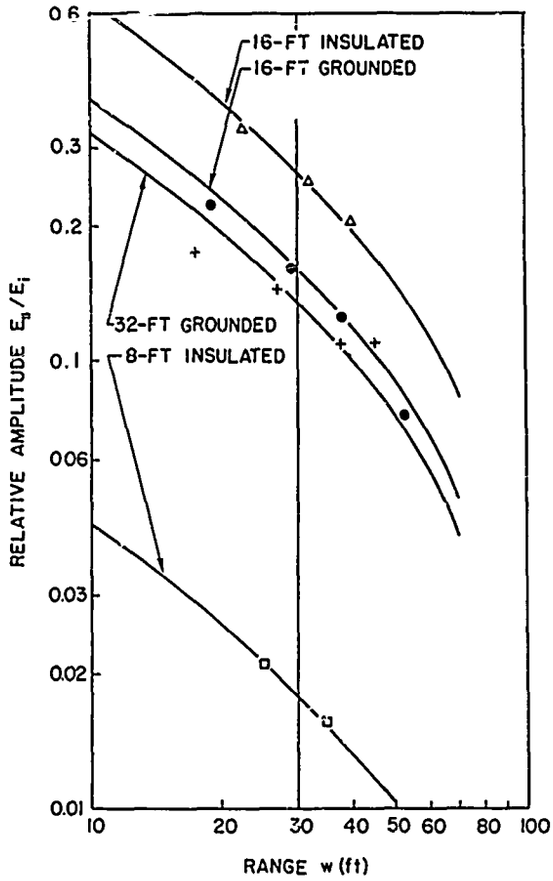

FIG. 13. RELATIVE AMPLITUDE OF BACKSCATTERED FIELD FOR VERTICAL CYLINDERS OF VARIOUS LENGTHS WITH THE STANDARD RANGE-DEPENDENCE CURVE SUPERIMPOSED.

itself had 5 ft of vertical extent, what was actually measured was

$$\int_{h-2.5}^{h+2.5} G \, dh \, ,$$

denoted J, which was equal to E_i^2 when $h = 8$. Figure 14 is a graph of J vs h.

An illumination factor I_L was defined as the ratio of the average power per unit area received by a target of length L to the average

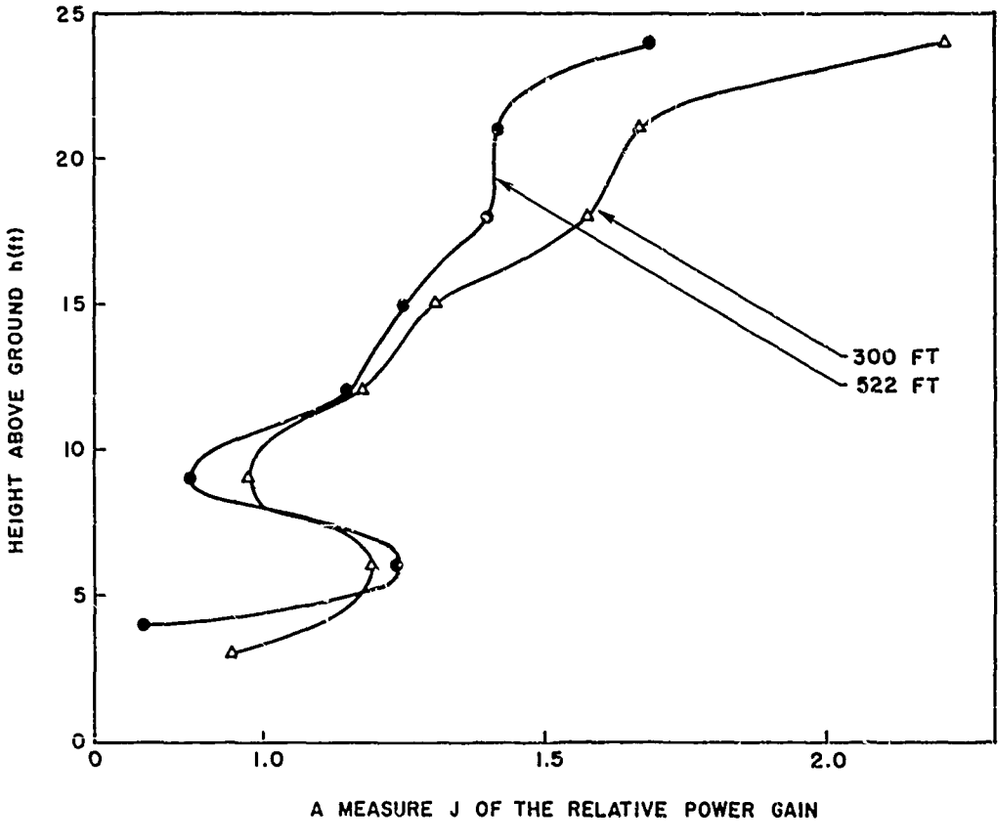

FIG. 14. RELATIVE POWER GAIN OF TRANSMITTING ANTENNA AT VARIOUS HEIGHTS ABOVE THE GROUND, FOR VERTICAL POLARIZATION.

power per unit area received by the probe of length 5 ft with its center 8 ft above the ground. Therefore

$$I_L = \frac{\frac{1}{L}\int_0^L G\, dh}{\frac{1}{5}\int_{5.5}^{10.5} G\, dh},$$

and the relative cross section is B/I_L.

At height h, G may be obtained approximately from Fig. 14 by putting

$$G = \frac{1}{5}\int_{h-2.5}^{h+2.5} G\, dh .$$

Then the integral in the numerator of I_L can be obtained by integrating G by a graphical method. The integral in the denominator of I_L is obtained from Fig. 14 at h = 8 ft. The factors I_L are shown in Fig. 15 for different target ranges, but the difference between the two curves may not be significant.

The illumination factor I_L must be used with some caution. Strictly, it should only be used to deduce cross sections of vertical targets of uniform horizontal extent; for a tree, however, the diameter of the trunk varies from bottom to top. Moreover, a knowledge of the height of the target is implied, but for a tree the effective target

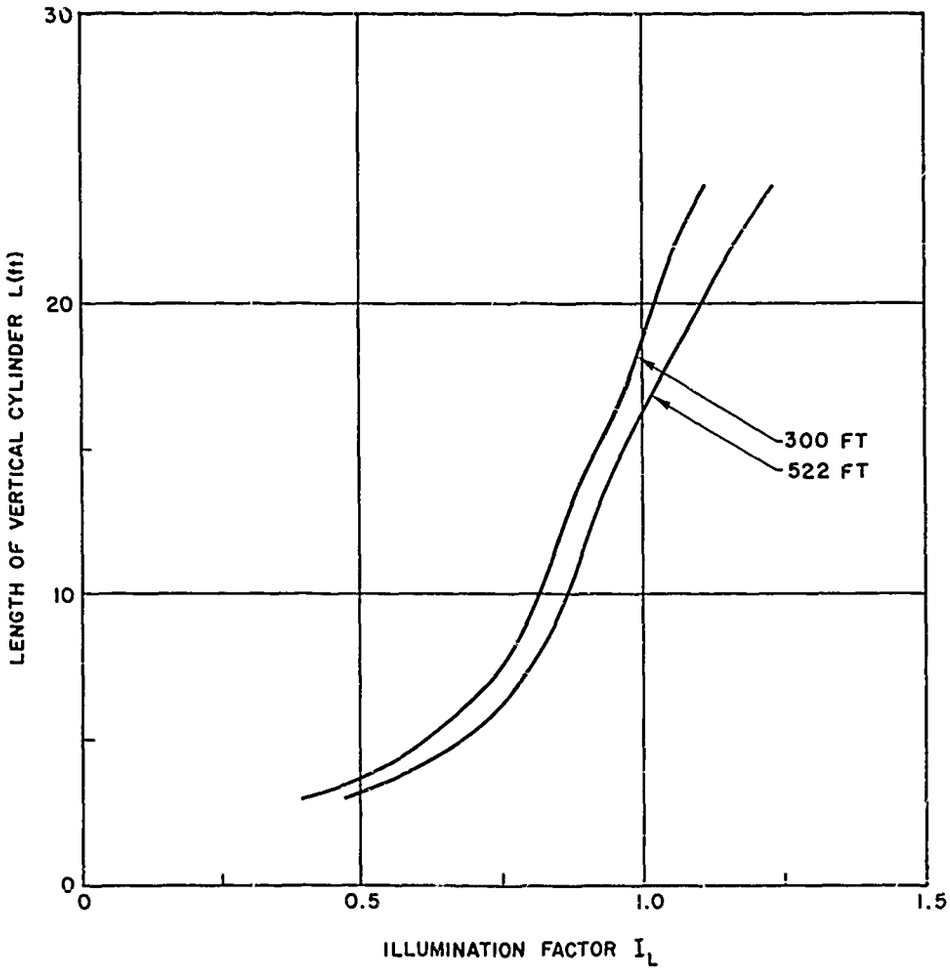

FIG. 15. ILLUMINATION FACTORS FOR VERTICAL POLARIZATION.

height may be quite different from the apparent height. In some cases this last difficulty may be overcome by deducing the effective height from the phase of the scattered field, as described in Chapter VI.

V. RESULTS FOR ALUMINUM DIPOLES

Intensive measurements were carried out using aluminum cylinders as targets. These measurements had a threefold purpose: to test the measurement technique under controlled conditions, to see how the results compared with earlier microwave results, and to calibrate the system so that results for B/I could be expressed in terms of σ.

As in all the work reported here, the wavelength λ was 38 ft. The aluminum cylinders were 3 in. in diameter, so that if $k = 2\pi/\lambda$ and a is the radius, $ka = 0.0207$. As the microwave results of Ås and Schmitt [Ref. 5] were not very sensitive to small changes in ka, we may expect our results to be comparable with theirs for $ka = 0.026$, and with those of Sevick [Ref. 4] for $ka = 0.022$.

The cylinders were investigated in three ways:

1. They were mounted horizontally at a height of 8 ft above the ground.
2. They were mounted vertically with one end on the ground but insulated from the ground by a piece of wood.
3. They were placed vertically on the ground and grounded by means of a sheet of chicken wire spread on the ground.

In all cases the polarization of the radiation was parallel to the axis of the target.

Relative cross sections for horizontal cylinders of various lengths are plotted in Fig. 16. A resonance peak appeared for a cylinder 17 ft long. This cylinder behaves as a half-wave dipole with $2h = 17$ ft, where h is the half-length of the dipole. Below 10 ft, the cross section was so small that the standing-wave amplitude was about the same as the random variations in the field caused by distant targets.

For insulated vertical cylinders, the illumination factor I_L was applied and the result, shown in Fig. 17, was quite similar to the horizontal case. To a first approximation, this similarity validates the assumptions regarding range dependence and illumination factors. The resonance peak occurred for a 16-ft cylinder. Perhaps the proximity to the ground causes an increase in the effective length of the target, so that a 16-ft cylinder with one end near the ground behaves like a 17-ft horizontal cylinder 8 ft above the ground.

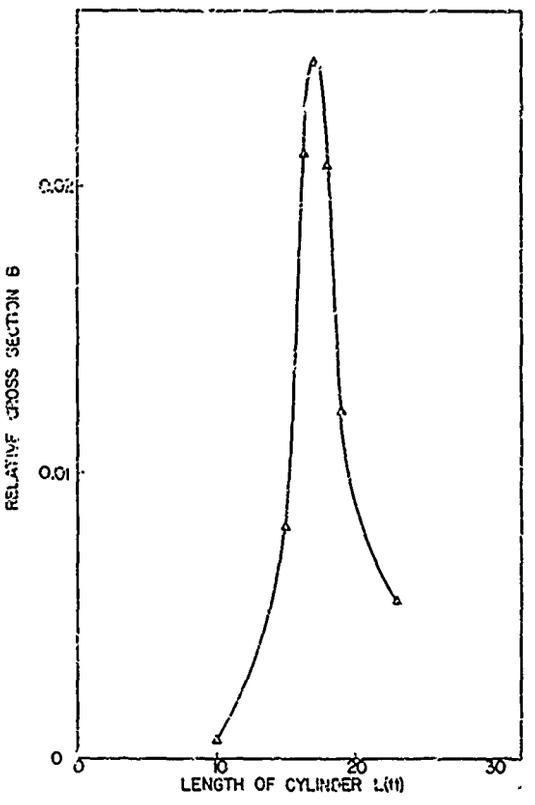

FIG. 16. RELATIVE CROSS SECTIONS FOR HORIZONTAL CYLINDERS OF VARIOUS LENGTHS.

The grounded vertical cylinders gave the result shown in Fig. 17. The first resonance peak appeared at 9 ft and a second peak emerged at about 29 ft. Grounding the targets doubled their effective lengths, so that a 9-ft cylinder behaved as a resonant dipole for which $2h = 18$ ft. This was nearer to the actual length of a half-wave dipole at 25.9 Mc than either of the insulated cases. The relative cross section at the first maximum was about half that for the insulated vertical dipole. This was probably because, after illumination factors had been taken into account to equalize the power density, a 9-ft cylinder captured about half the power received by a 16-ft cylinder when both acted as half-wave dipoles (that is, $2h = \lambda/2$). The possibility of power losses in the grounded case is discussed at the end of this chapter. The chicken wire caused a standing wave of its own, even after the cylinders were removed, but usually its amplitude was small enough to be neglected.

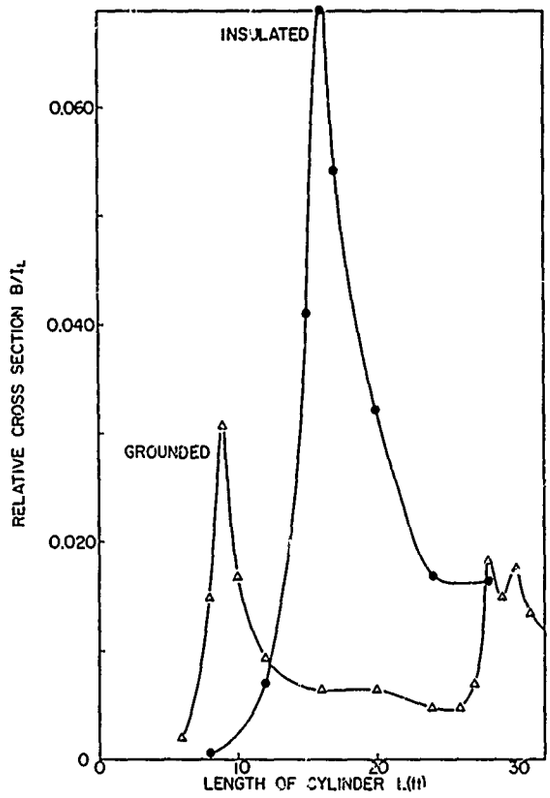

FIG. 17. RELATIVE CROSS SECTIONS FOR VERTICAL CYLINDERS OF VARIOUS LENGTHS.

It will now be of interest to compare the results of Figs. 16 and 17 with one another and with earlier microwave results. Figure 18 shows the microwave results of Ås and Schmitt [Ref. 5] and Sevick [Ref. 4] translated to 25.9 Mc. Also shown is the curve for grounded cylinders, replotted from Fig. 17 in terms of $2h$ instead of L, and moved up the page to make $\sigma/\lambda^2 = 0.88$ for the first resonance peak. The agreement between curves (b) and (c) reinforces the belief that the present adaptation of the standing-wave method is sound, and conversely, shows that microwave results can confidently be extrapolated to the high-frequency region, with implications discussed in Chapter VIII.

The discrepancy between curves (b) and (c) for $2h = 12$ ft may be due to an error in I_L when $L = 6$ ft, since the illumination factors are considered to be least accurate for small values of L. The discrepancies above $2h = 40$ ft may be due in part to errors in I_L, since

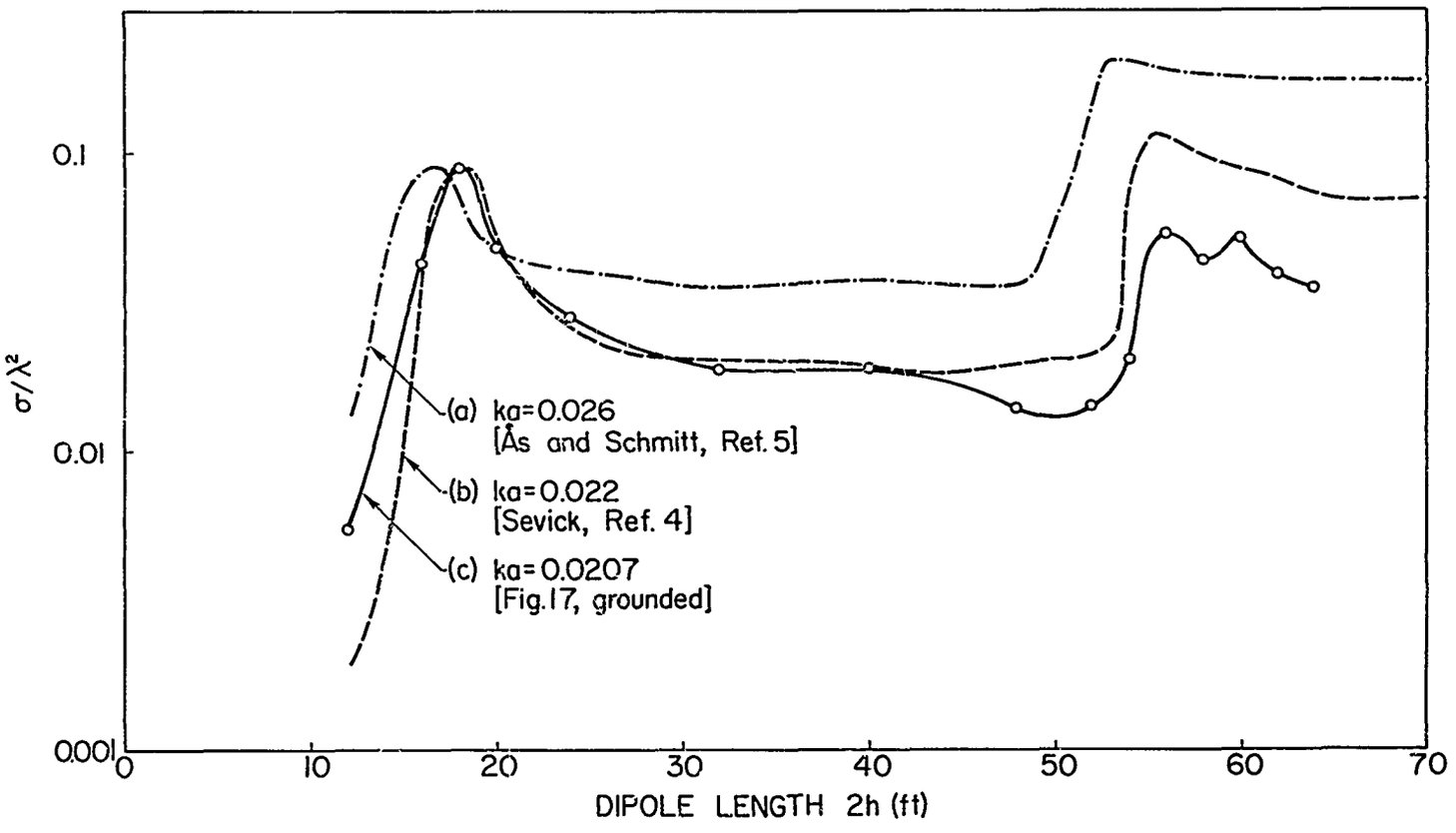

FIG. 18. CROSS SECTIONS OF DIPOLES.

I_L was measured only up to L = 24 ft, but, more likely, to the increasing angle subtended at the probe by the target, so that the scattered radiation reaching the probe had a spherical wavefront at the target. As mentioned in Chapter I, this could give rise to measured values of cross section perhaps 10 percent too small. In an effort to combat this problem, the standard curve used in data reduction was fitted preferentially to points of large range from the target.

A further factor contributing to the discrepancies between curves (b) and (c) above 40 ft may be that ka is smaller for (c) than for (b). The results of Ås and Schmitt [Ref. 5] for various values of ka show that σ/λ^2 decreases with smaller ka, except at the first resonance peak. This result may also partly explain the difference between curves (a) and (b).

The three curves of Figs. 16 and 17 are compared in Fig. 19. Again the first resonance peak for each curve was placed at $\sigma/\lambda^2 = 0.88$, and apart from the difference in resonant lengths, the curves are quite similar.

The agreement of the present results with those obtained from microwave measurements (which agree in turn with approximate theoretical results [Ref. 8]) offers a reliable method of calibrating the present results. Using the fact that $\sigma/\lambda^2 = 0.88$ at the first resonance peak, we can deduce a constant of proportionality to link B/I to σ for each of the three classes of targets examined. The constant for the grounded vertical cylinders should also serve for targets such as trees, since the root system of a tree should serve as a ground plane with good radio-frequency coupling to the earth.

In addition to the three classes of targets referred to above, poorly grounded vertical cylinders were used as targets. The cylinders were simply placed on the earth without any chicken-wire screen. The results were not always repeatable inasmuch as the effectiveness of grounding varied with the moisture content of the soil. Relative cross sections were about half those for insulated vertical cylinders of equivalent length, and decreased with increasing moisture.

In addition to cross sections, the phase ϕ of the target reflection coefficient was obtained from the data. Referring to Fig. 10, if the phase

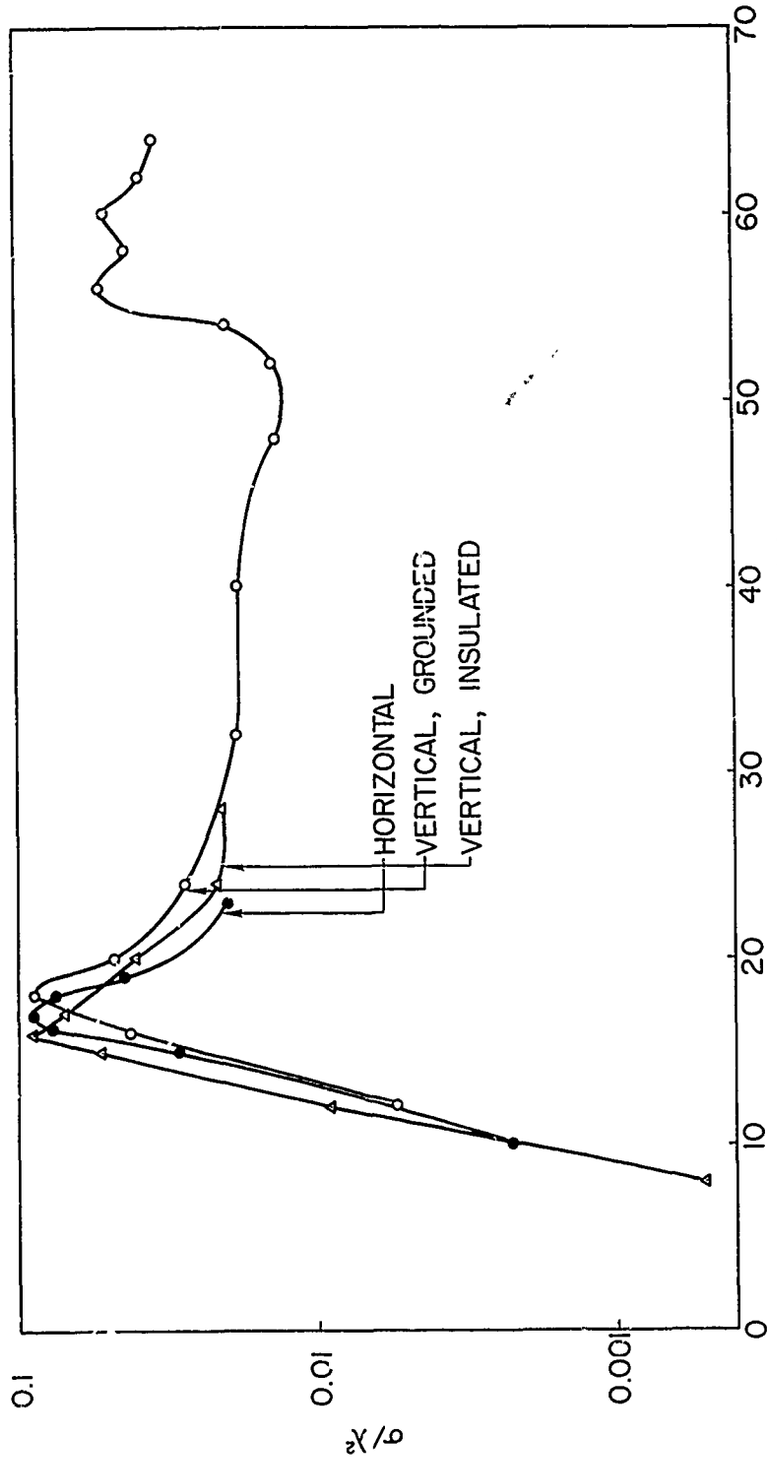

FIG. 19. CROSS SECTIONS OF DIPOLES, FROM FIGS. 16 AND 17.

change on reflection was 180 deg, the minima would occur at integral multiples of $\lambda/2$ (19 ft) from the target. In general, the minima were displaced from these positions by an amount w_1, signifying that the phase ϕ was $2kw_1$ radians (or $19w_1$ deg) less than 180 deg. For example, in Fig. 10a, w_1 = 5 ft and so ϕ was 180 - 95 deg, or 85 deg. As this is close to 90 deg, it is consistent with the usual behavior of a resonant dipole.

Figure 20 is a graph of ϕ vs cylinder length L for the three classes of targets, labeled as in Figs. 16 to 19. The horizontal polarization curve compares well with one of the curves in Fig. 6 of King [Ref. 3].

The vertical polarization curves agree with one another if they are plotted against 2h instead of L. The second resonance peak of the grounded curve in Fig. 17 has its counterpart in the positive gradient of the grounded curve in Fig. 20. The minimum point of Fig. 17 is reflected in the negative gradient of Fig. 20. However, there is an error in the vertical curves of Fig. 20; their phase values are too high. For example, at resonance ϕ is about 160 deg instead of 90 deg. This difference is presumably because the ground between the target and the probe introduces a further change in the phase of the scattered radiation reaching the probe. Below the Brewster angle for ground reflection, the phase of the reflection coefficient varies between 90 deg and 180 deg, and the component of the scattered energy reaching the probe by reflection from the ground may be, say, 140 deg out of phase with the direct component. The resultant of the two components is perhaps 50 deg out of phase with the direct component. Such a further change does not occur for horizontal polarization, since--provided the probe is far enough from the target--the two components of scattered radiation reaching the probe are out of phase by nearly 180 deg and the resultant has almost the same phase as the larger (direct) component.

The curves of Fig. 20 may be used for estimating the effective length of a target, as discussed in Chapter VI. The error in ϕ is not a problem, as the length may be read directly from the values of w_1 at the right-hand side of Fig. 20.

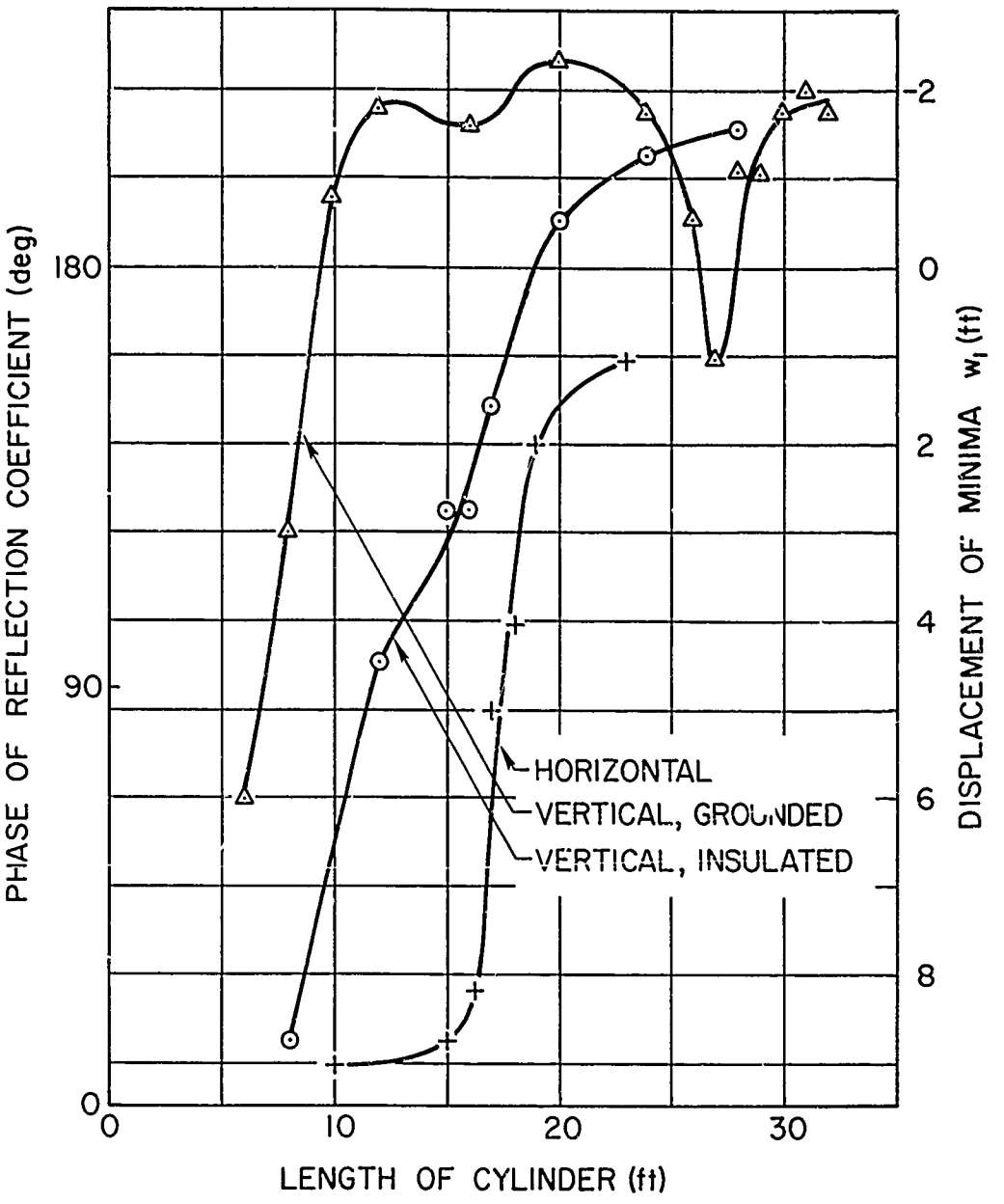

FIG. 20. DISPLACEMENT OF THE STANDING-WAVE MINIMA.

In the work described so far, the axis of the target was perpendicular to the direction of propagation. To investigate how much the relative cross section was sensitive to variations from this alignment, certain measurements of cross sections of horizontal cylinders were repeated, with the target axis deflected at various angles θ from the

normal to the propagation direction. The number of measurements was insufficient to enable a detailed analysis to be made, but the results, illustrated in Fig. 21, show that, for deflection angles close to zero, B changes by 1 or 2 percent per degree of deflection.

The curves of Fig. 21 may be regarded as reception-radiation patterns of the targets, or the square of the radiation patterns. For example, an elementary dipole with a radiation pattern described by $\cos^2 \theta$ may have a reception-radiation pattern $B(\theta)$ proportional to

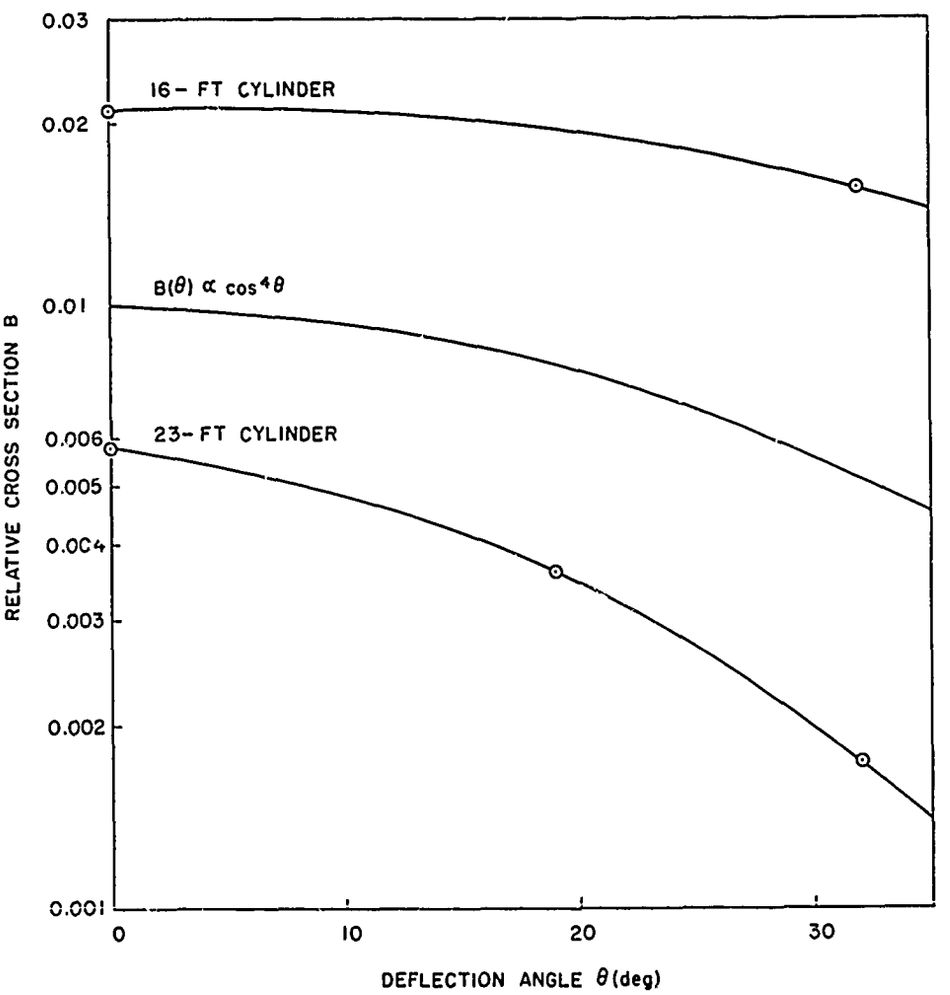

FIG. 21. RELATIVE CROSS SECTIONS OF HORIZONTAL CYLINDERS DEFLECTED THROUGH AN ANGLE $B(\theta)$ FROM NORMAL TO THE DIRECTION OF PROPAGATION.

$\cos^4 \theta$, and this function is shown in Fig. 21 for comparison with the experimental results for cylinders 16 ft and 23 ft long. Half-power beamwidths for $B(\theta)$ (that is, for reception and subsequent transmission) were 23 deg for the 23-ft cylinder, and perhaps 45 deg for the 16-ft cylinder.

As mentioned earlier in this chapter, a possible reason for the relative cross section of the resonant grounded cylinder being smaller than that of the resonant insulated vertical cylinder is that absorptive losses occurred in the grounded case. It is conceivable that currents flowing in the ground dissipated half the energy received by the cylinder before it could be transmitted.

Absorptive losses would be expected to affect the curves of Figs. 19 and 20 as illustrated in Fig. 6 of King's paper [Ref. 3]. Such losses would cause a flattening of the resonance peaks, but Fig. 19 does not indicate this; the height and width of the first resonance peak is the same for both vertical curves. Losses would also suppress the resonance behavior of the phase curves of Fig. 20, but in fact, apart from the factor of 2 in the ordinate, the vertical curves are identical. It may be concluded that any losses are quite small.

VI. RESULTS FOR TREES

The standing-wave method is applicable if the range to the target has a discrete value. A tree may have limbs which spread 30 ft or more from the trunk, so that at 25.9 Mc the diameter to the outer leaves may be considerably more than a wavelength. The various parts of the tree all contribute standing waves in different phase relationships. If the parts were uniformly distributed throughout the volume occupied by the tree, the various standing waves would tend to cancel each other out.

Fortunately for the present purpose, the main scatterers of a tree are concentrated within a few feet of its geometric center. It is expected that the cross section of a branch is proportional to the square of its volume [Wetzel, Ref. 9]. Hence, for vertical polarization, the contributions of several large vertical branches will be only a few percent of that of the trunk. For horizontal polarization, the trunk, being vertical, may contribute little, but any horizontal branches roughly perpendicular to the direction of illumination will contribute, and such branches will exist mainly at the same range as the trunk. These expectations are largely fulfilled in the work to be described.

Three oak trees were used as targets. They are labeled I, II, and III in the aerial photograph of Fig. 2 and are shown separately in Figs. 22 through 26. Tree I was chosen because it is well separated from other trees; its isolation, in fact, was the original reason for the choice of the site. It is about 35 ft high and 60 ft in diameter, with a trunk about 4 ft in diameter. Tree II is not as well isolated, but is larger than other trees in its vicinity; it is 40 ft high and its trunk diameter is similar to that of Tree I. Tree III is fairly well isolated and is smaller than I or II.

For ease of presentation, Tree III will be discussed first. The standing-wave data are shown plotted in Fig. 27 for vertical polarization. The standing wave was particularly clear, as might be expected for a tree of small dimensions remote from other trees. Its amplitude was surprisingly large. Careful reduction of data showed that the quantity B was 0.0149. The relative cross section B/I_L requires a knowledge of L, the effective height of the tree.

FIG. 22. PHOTOGRAPH OF TREE I.

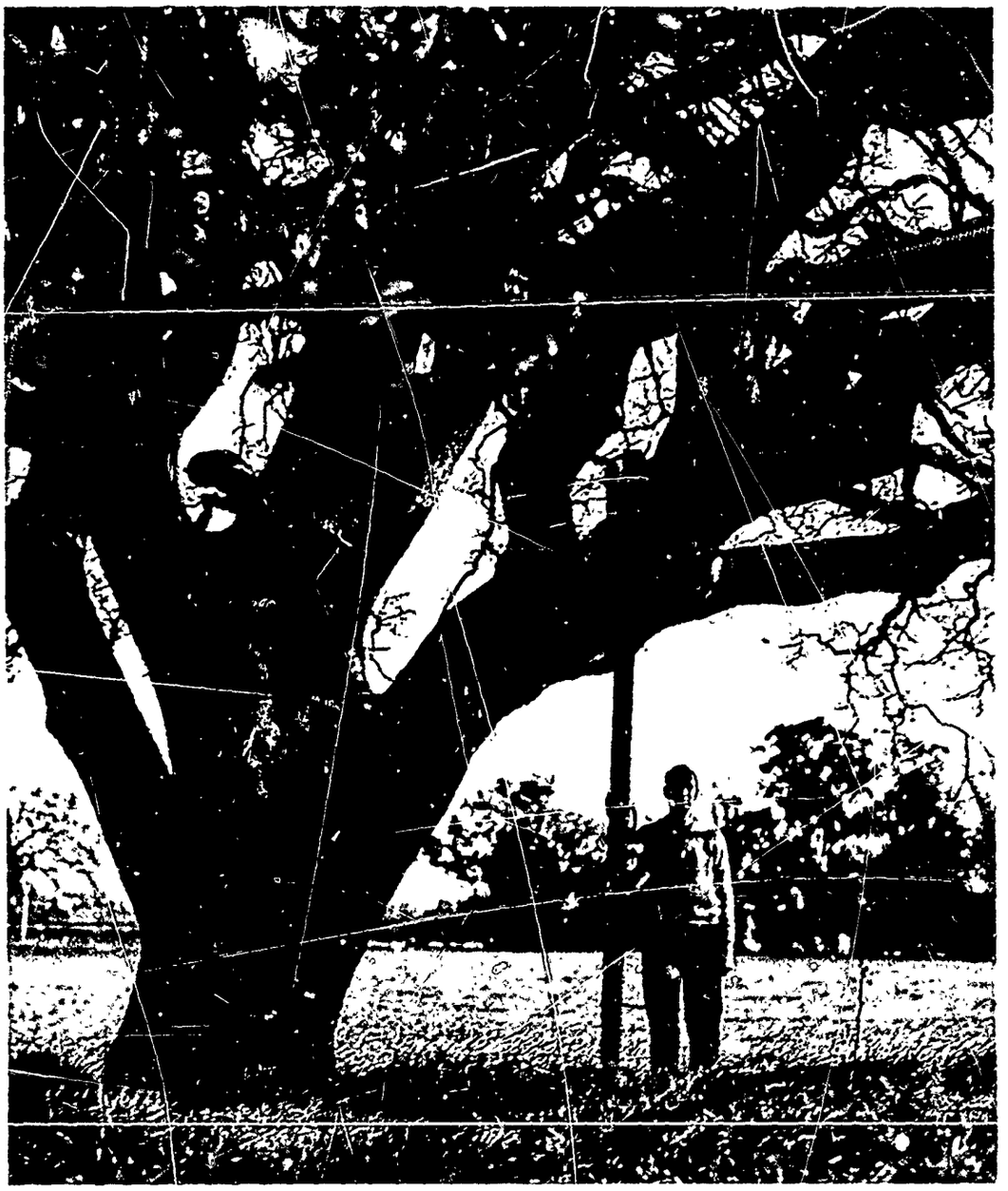

FIG. 23. CLOSEUP OF TREE I SHOWING TRUNK AND MAIN BRANCHES.

FIG. 24. PHOTOGRAPH OF TREE II.

FIG. 25. CLOSEUP OF TREE II.

FIG. 26. PHOTOGRAPH OF TREE III.

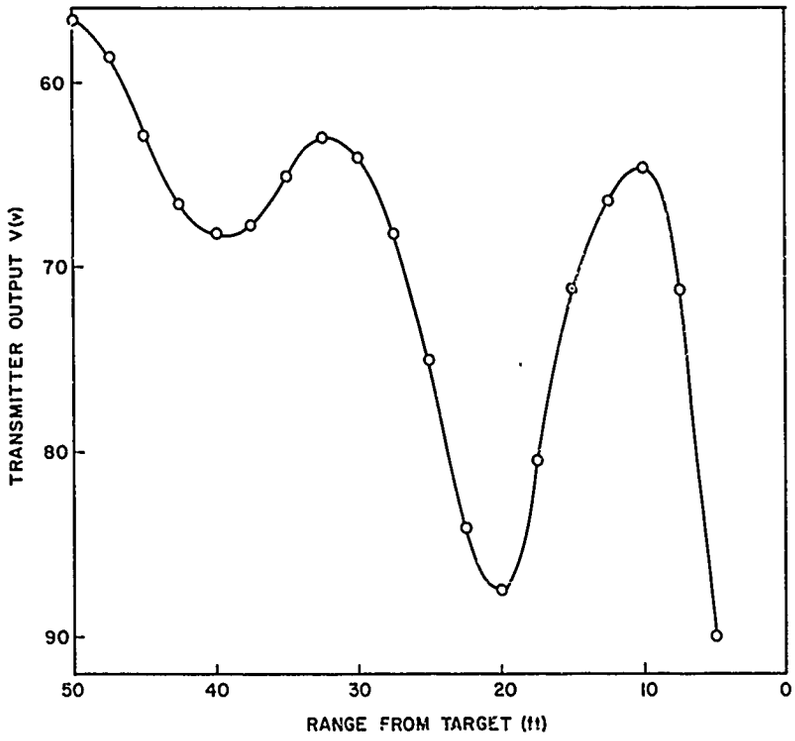

FIG. 27. STANDING-WAVE DATA FOR TREE III, VERTICAL POLARIZATION.

Let us assume that the grounded vertical curve of Fig. 20 can be applied to trees; this is a bold assumption, but it is strengthened as the argument proceeds. The displacement w_1 of the standing wave was 2.5 ft, and in Fig. 20 this corresponds to an effective height of 8 ft. The illumination factor I_L obtained from the 300-ft curve of Fig. 15 is 0.82, so B/I_L is 0.0182. This value is almost identical with that of B/I for an 8-ft aluminum cylinder (grounded curve of Fig. 17), which seems to strengthen the above assumption.

The cross section is obtained by using the first resonance peak of the grounded curve of Fig. 17 as a calibration standard. Since $\sigma/\lambda^2 = 0.88$ for this resonance peak, we have, for Tree III,

$$\sigma/\lambda^2 = \frac{0.0182}{0.0308} \times 0.88 = 0.52$$

At 25.9 Mc, $\lambda^2 = 134.5\ m^2$, so $\sigma = 70.0\ m^2$.

Since the effective height of 8 ft is close to the resonant length of 9 ft, the value of σ obtained here is probably larger than that for similar, nonresonant, trees.

It is of interest to compare the effective height with the tree structure. Figure 26 shows that the trunk forks at a height of about 7.5 ft. Perhaps the trunk extends for 0.5 ft below the ground. Since the portion of trunk below the fork can be identified with the main source of echo, the expectations are confirmed.

Now, let us consider Tree II. The standing-wave data are illustrated in Fig. 28 for vertical polarization. The curve is rather

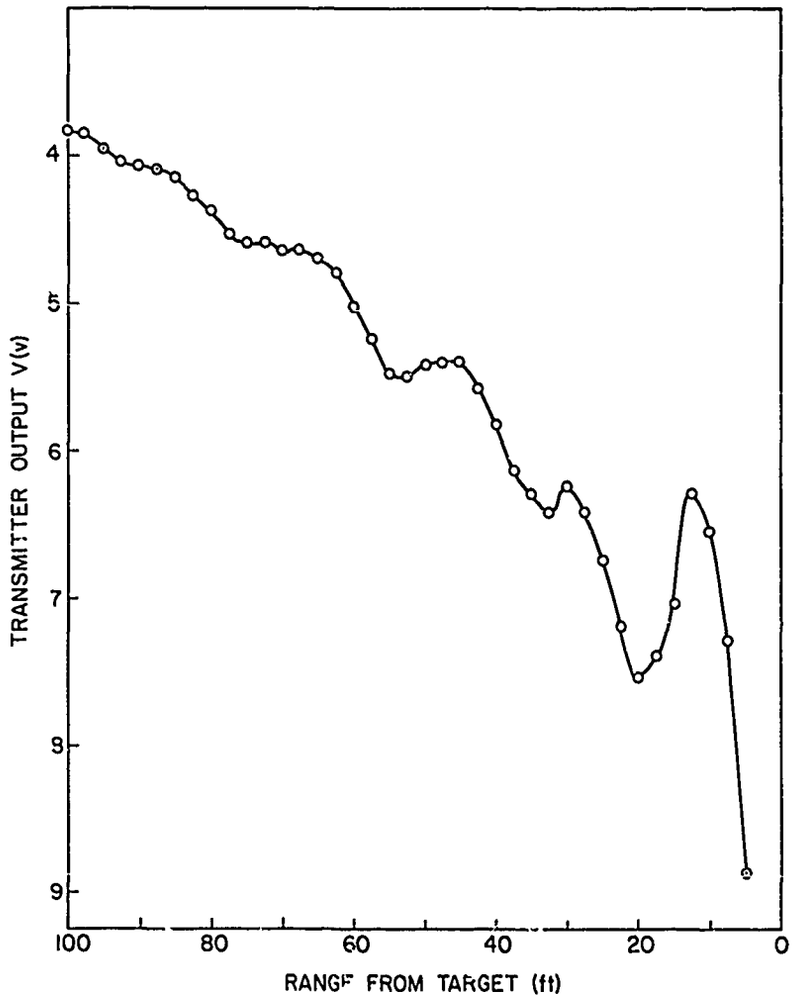

FIG. 28. STANDING-WAVE DATA FOR TREE II, VERTICAL POLARIZATION.

distorted close to the tree, for overhanging branches were sometimes only a matter of inches from the probe. Farther from the tree, distortions were probably due to contributions from other trees in the vicinity. The value of B obtained was 0.0156.

The height of the tree could not be deduced exactly from the vertical grounded curve of Fig. 20 since w_1 was -3 ft. It is probable that w_1 was actually -2, corresponding to any length from 12 to 24 ft, and that the remaining 1 ft means that the range from the probe to the effective center of the trunk is 1 ft greater than the range to the geometrical center of the base of the trunk. Such a probability might occur if the main echoing branch of the trunk had this range, or if it were high enough to have an oblique range equal to this. In any case, it may be assumed that L is between 12 and 24 ft, so that I_L, from the 300-ft curve of Fig. 15, is between 0.9 and 1.24 and B/I_L is between 0.0173 and 0.0126.

Calibrating as before, we obtain the result that, for Tree II, σ is between 66.5 and 48.4 m^2.

Tree I gave a result similar to Tree II; its data are plotted in Fig. 29a for vertical polarization. Since the radius of the tree to the outer leaves was 35 ft, some of the points represent readings taken when the probe was beneath or among the branches, but the standing wave due to the trunk was still dominant. The value of B was 0.00883, and that for w_1 was -3. Using the 522-ft curve of Fig. 15 and assuming the same values of L as for Tree II, we arrive at values of σ between 40.0 and 30.6 m^2.

Data were also obtained for horizontal polarization in the case of Tree I and these are plotted in Fig. 29b. The probe, when horizontally polarized, could not be moved among the branches, owing to lack of space, and therefore data could be obtained only for ranges greater than 35 ft from the trunk. The value of B was 0.0256; that for w_1 was zero. We are not helped much by knowing w_1, but the horizontal polarization curve in Fig. 20 does indicate that the effective horizontal length is greater than 23 ft and probably several feet less than the second resonant length of about 50 ft. An estimate would be 30 ft, which is half the outer diameter of the tree, and this estimate agrees with the apparent result that the effective height is about half the total height.

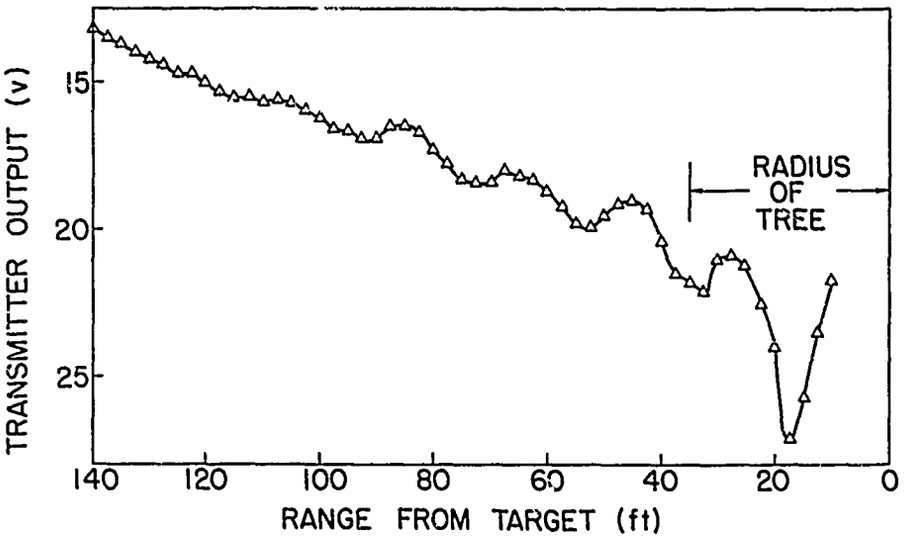

a. Vertical polarization

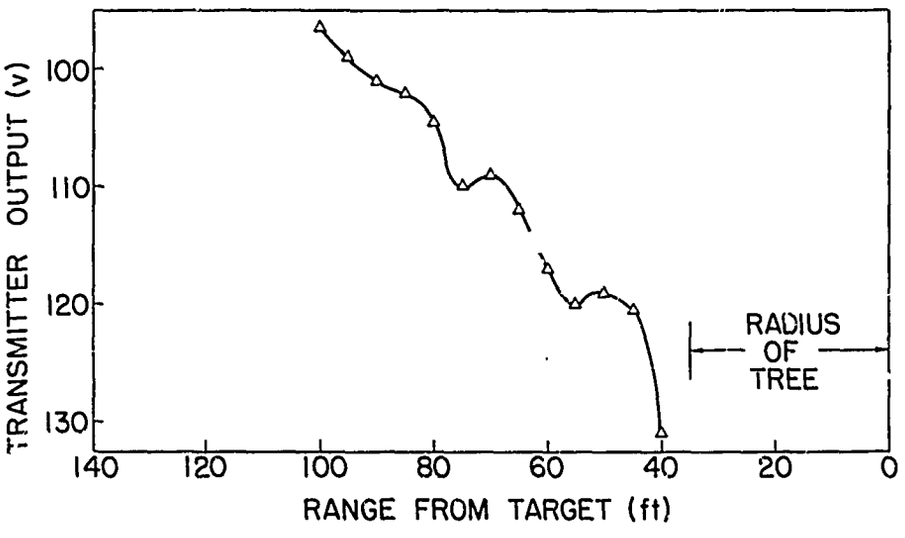

b. Horizontal polarization

FIG. 29. STANDING-WAVE DATA FOR TREE I.

For the illumination factor it is necessary to estimate the effective height of the largest horizontal branches. Suppose the effective height is 13 ft, as seems likely from Fig. 23. Then, from Fig. 13, I_h is 2.35. Actually the target-transmitter range was not 300 ft but

522 ft, so Fig. 13 is not quite applicable here, but any error would not be large for values of h close to 8 ft.

After calibrating with reference to the resonance peak of Fig. 16, we obtain $\sigma = 53.0\ m^2$. It is interesting to note that this is larger than the cross section of the same tree with vertical polarization. However, because of the large approximations made in deriving both results, it is preferable to conclude that the cross sections for horizontal and vertical polarizations are of the same order of magnitude for this oak tree.

Table 4 summarizes the main results described in this chapter.

TABLE 4. PARAMETERS USED IN CALCULATING CROSS SECTIONS OF TREES

Tree	Polarization	B	w_1 (ft)	L (ft)	I	Calibration Factor	σ (m^2)
III	V	0.0149	2.5	8	0.82	0.0308	70.0
II	V	0.0156	-3	12-24	0.9 -1.24	0.0308	66.5-48.4
I	V	0.00883	-3	12-24	0.85-1.11	0.0308	40.0-30.6
I	H	0.0256	0	~30	~2.35	0.0243	~53.0

VII. RESULTS FOR STREET LIGHTS AND VEHICLES

The radar targets most likely to aid in the identification of highways and developed areas are probably street lights (electroliers) and vehicles. The former are easily treated by the techniques developed for aluminum cylinders; the latter are more difficult to deal with because of their three-dimensional shapes. The results obtained are listed in Table 5 for vertical polarization, and will be discussed in the same order.

TABLE 5. PARAMETERS USED IN CALCULATING CROSS SECTIONS OF STREET LIGHTS AND VEHICLES FOR VERTICAL POLARIZATION

Target	Aspect	B	L (ft)	I_L	Calibration Factor	σ (m^2)
Street light	--	0.198	28.5	1.4	0.0694	241
Antenna mast	--	0.031	55.5	1.2	0.0694	44
Small car	broadside	0.00336	4.8	0.685	0.0694	8.35
Jeep	broadside 45°	0.00336	5.6	0.735	0.0694	7.78
Truck	broadside 45° rear end	0.0144 0.001025 0.00038	10.7	0.88	0.0694	27.9 1.98 0.736

The street light and the antenna mast were both grounded in the sense that they had good direct-current connections to the earth. But, unlike the aluminum cylinders described as "grounded" in Chapter V, these targets had no metal ground plane at the base and the question arose as to whether the calibration factor would be appropriate for grounded or for insulated vertical cylinders.

The question was resolved by referring to the curves of w_1 vs L in Fig. 20. Table 6 compares the w_1 values of Fig. 20 for insulated

and "grounded" cylinders of the given lengths with the measured values of w_1. For this purpose, the insulated curve was extrapolated to higher values of L by doubling the L scale of the grounded curve.

TABLE 6. DISPLACEMENT OF STANDING-WAVE MINIMA

Target	From Measurement		From Fig. 20	
			Grounded	Insulated
	L (ft)	w_1 (ft)	w_1 (ft)	w_1 (ft)
Street light	28.5	-2.75	-1	-2
Antenna mast	55.5	0.5	-2	0.5

The "insulated" values agree fairly well with the measurements, so it will be concluded that these targets behave like the insulated cylinders of Chapter V, with appropriate calibration factors and similar resonance behavior. This means that the antenna mast is close to a resonant length, and the street light is about halfway between resonances (see Fig. 19). We would therefore expect the antenna mast to have the larger cross section of the two, but in Table 5 such is not the case. Perhaps, as found for the "poorly grounded cylinders" in Chapter V, the cross section depends on the effectiveness of the grounding.

The street light, which is shown in Fig. 30, was tapered from a diameter of 8.3 in. just above the pedestal to about 6 in. at the top. This means that the illumination factor is slightly in error. The antenna mast was also tapered, but a more serious approximation was the extrapolation of the illumination factor to a height of 55.5 ft, since it was measured only to 30 ft. The curve that was extrapolated is not shown in Fig. 15, but it was less steep than either of those shown.

The car and the jeep were similar in cross section, and did not exhibit any marked aspect sensitivity. Illumination factors appropriate to vertical cylinders were even less applicable than before but were nevertheless used for want of better figures. The calibration factor chosen was the one for vertical targets insulated from the ground.

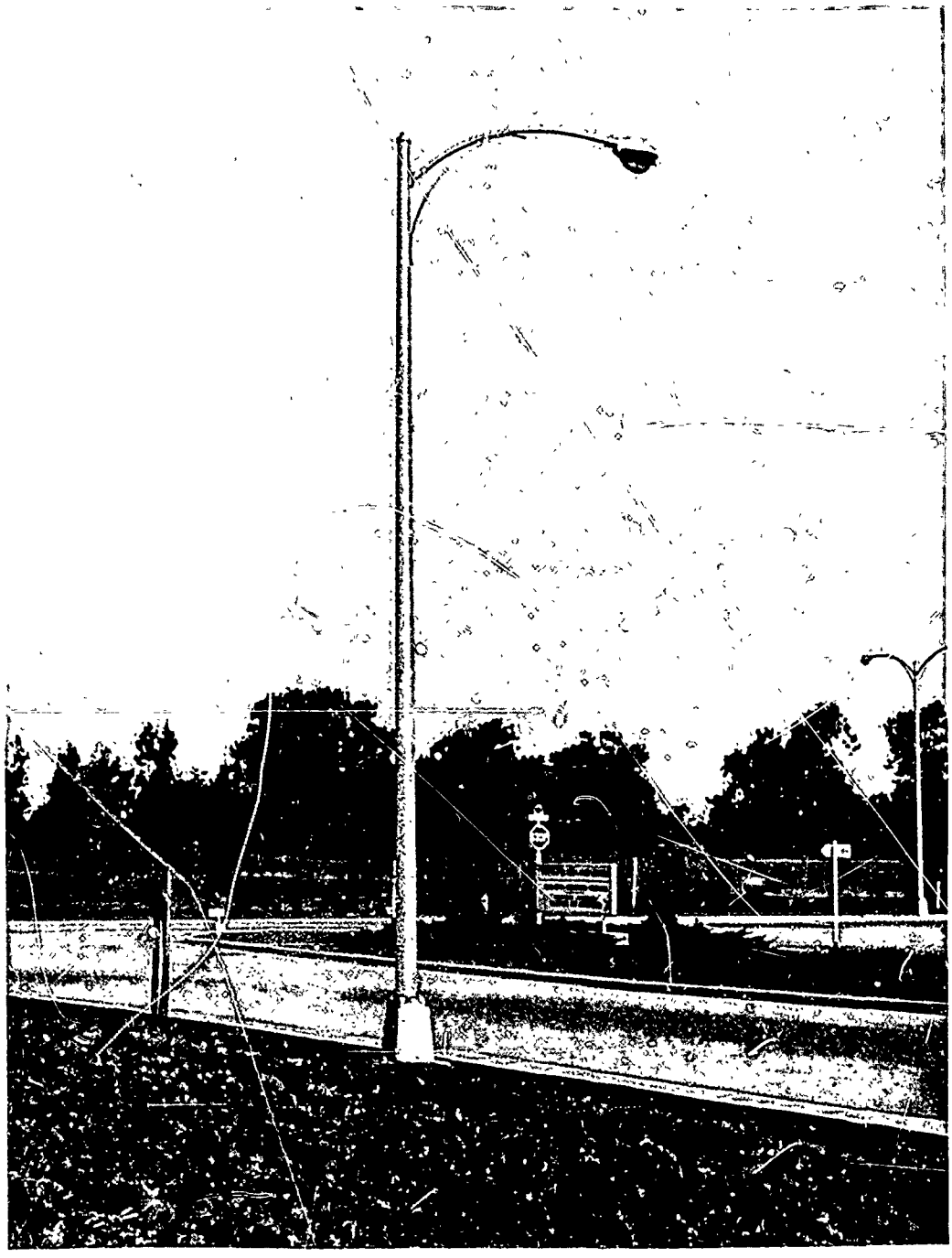

FIG. 30. STREET LIGHT USED AS A RADAR TARGET.

The dimensions of the truck are shown in Fig. 31. While the shape of the truck is fairly simple, being largely a rectangular box, as a radar target at 25.9 Mc it is quite complicated. Currents induced in

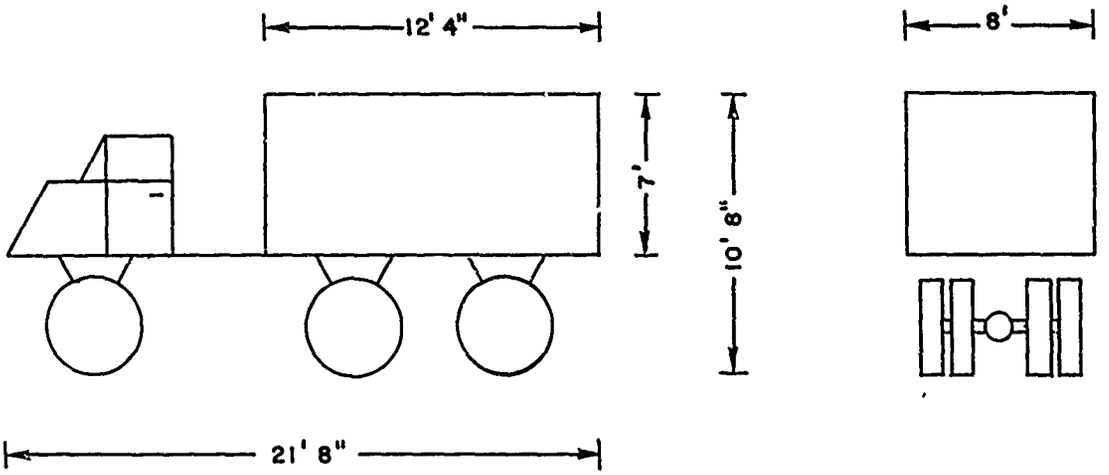

FIG. 31. DIMENSIONS OF TRUCK USED AS A RADAR TARGET.

the metal structure may flow in three dimensions instead of the one dimension assumed for vertical cylinders. The radiation from the truck is far from isotropic, because the dimensions are not small compared to a wavelength. The cross section is therefore very aspect sensitive. As might be expected, it is largest in the broadside direction and has a very small value when the truck is viewed from the rear--smaller, in fact, than the cross section of a small car or jeep. Figure 32 compares the radar cross sections of a small car and a truck, showing typical angular dependence at 25.9 Mc.

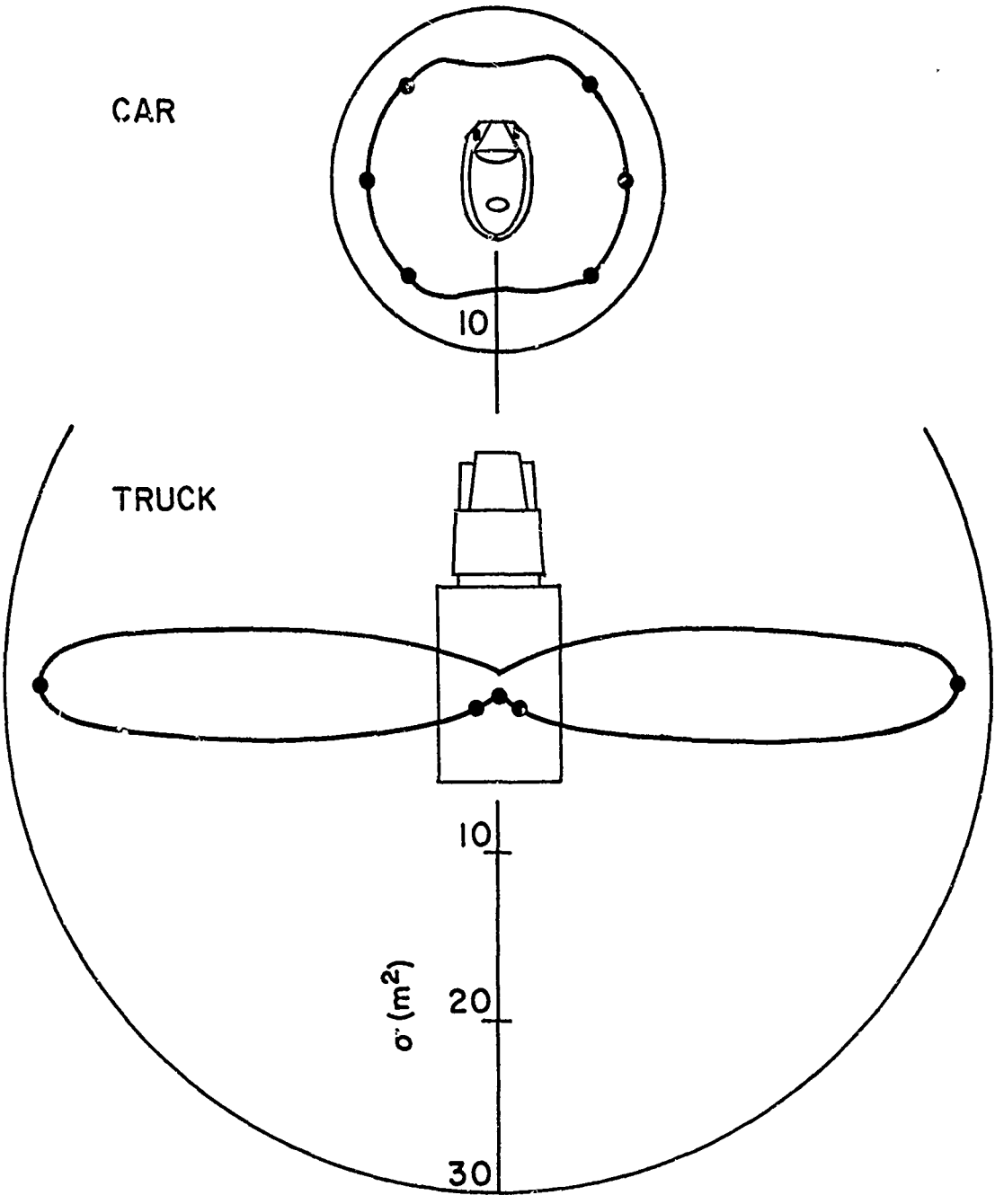

FIG. 32. VARIATION OF CROSS SECTION WITH ASPECT ANGLE FOR VEHICLES.

VIII. EXTRAPOLATION OF MICROWAVE RESULTS TO HIGH FREQUENCY

Microwave results for conducting cylinders or dipoles are generally presented as a curve of σ/λ^2 vs kh, where $k = 2\pi/\lambda$ and h is the half-length of a dipole [Ref. 8]. This presentation implies that the results obtained at a wavelength of 10 cm are applicable at other wavelengths by substituting the relevant wave number. This extrapolation procedure was followed to obtain curves (a) and (b) of Fig. 18, and their close correspondence with the high-frequency results at 11.6 m justifies the procedure.

This extrapolation involved a wavelength multiplication of over 100. The success of the extrapolation suggests that it can be carried further by another factor of 10, to the extreme long-wave end of the high-frequency spectrum. Indeed, there seems to be no reason why the curve should not apply at any frequency at all.

It may be of interest to know at what frequencies in the high-frequency range a conducting cylinder of given length exhibits resonance. Suppose we consider a cylinder 50 ft long, so that h is 25 ft. Then $kh = 150/\lambda$ approximately, or $f/2$, where f is the frequency in megacycles. We then have $f = 2kh$.

For the given cylinder length, then, the graph of σ/λ^2 vs kh, where kh may range from 0 to 12 (as for example Fig. 47 in Ref. 8), is also a graph of σ/λ^2 vs f from 0 to 24 Mc, and it is easily seen that the resonances occur for f = 3, 9, 15.5, and 21.5 Mc. If kh is large, the resonance peaks become small compared to the background, and σ/λ^2 is approximately proportional to $(kh)^2$; hence σ is proportional to h^2, which is independent of the frequency. This result agrees with the theoretical result quoted by Kerr [page 461, Ref. 10]. One interesting application of this case at high frequency is a power line; its cross section should be very large at broadside incidence.

For a tree of height 50 ft, the effective height may be about 25 ft, and with the assumption that it is like a grounded cylinder with a conducting ground plane, h is 25 ft, and again the resonances occur at frequencies of 3, 9, 15.5, and 21.5 Mc. However, it is not usually possible to know what the effective height of a tree is, and it is

probably more useful to consider a large number of trees of different effective heights. At any frequency above the lowest resonance frequency for the largest tree, some trees will resonate and others will not, so the curve of σ/λ^2 vs f becomes smoothed out, leaving a curve of a form $\sigma/\lambda^2 \propto f^2$. This means that for a given assembly of scatterers of random heights, the cross section is approximately constant as the frequency varies above the lowest resonance.

For a metal street light such as was discussed in Chapter VII, if the height is 25 ft, h is 12.5 ft, and the first two resonance peaks occur at 6 and 18 Mc (to mention only those in the high-frequency range). If a town or highway has many street lights of the same height, the backscatter coefficient of the region should be quite sensitive to frequency. Referring again to Fig. 47 in Ref. 8, we note that the first and second resonance peaks are about 10 db and 5 db respectively above the nonresonant background. This means that if only street lights 25 ft high are present, echo enhancements of 10 db at about 6 Mc, and 5 db at 18 Mc, should occur.

IX. RELEVANCE TO GROUND BACKSCATTER

Ground-backscatter coefficients measured by the standing-wave method will be the subject of a future report [Ref. 11], but since the results described in the present report have interesting implications for ground backscatter, they are discussed briefly in this chapter.

The present results are for targets in free space; for a vertical target on the ground, illuminated from an angle of elevation equal to the Brewster angle for the particular ground, the cross section for vertical polarization should be approximately equal to the free-space value modified by an obliquity factor. This is because, at the Brewster angle, the ground-reflection coefficient for vertical polarization is small (perhaps 0.2 at high frequency). The target is illuminated almost as if it were in free space and inclined at the Brewster angle to the incident wavefronts. If the angle is, say, 15 deg, Fig. 21 suggests that the cross section will be about 86 percent of its value when the angle is zero.

For example, let us suppose that a tree has a free-space cross section of 50 m^2 in the broadside direction. The same tree on the ground, illuminated at an angle of elevation equal to the Brewster angle, would have a cross section of perhaps 43 m^2. This would be quite a typical value for angles of elevation equal to and greater than the Brewster angle, since both theory [Refs. 9, 12] and experiment [Refs. 1, 2] have shown that the backscatter coefficient for vertical polarization remains fairly constant over such a range of angles.

The cross section would, of course, also depend on the size and type of trees and the wavelength of the radiation; and the backscatter coefficient, or cross section per unit area of the ground, would further depend on the area density of trees. Trees with effective heights much less than the resonant length of $\lambda/4$ would have a very small cross section. If the effective height is typically half the total height H, the requirement for appreciable backscatter is that H should not be much less than $\lambda/2$. For example, at 25.9 Mc it is required that the total height should not be much less than 19 ft.

Theoretical calculations by Wetzel [Ref. 9], developed by Basler and Scott [Ref. 13], predict that, for a tree of diameter 1.5 ft standing on the ground, the cross section for angles of elevation near the Brewster angle is between 0.01 and 0.1 m^2, which is three orders of magnitude smaller than the value suggested here. The trees used in the present experiment had diameters two or three times as large as was assumed by Wetzel. If, as Wetzel says, the cross section is proportional to the square of the volume, we arrive at a factor of 260 or so, which may account for the three orders of magnitude.

It should be noted that, whereas in Chapter VI the cross section of Tree I was approximately the same for both horizontal and vertical polarizations when the tree was effectively in free space, this would not be true for a tree on the ground viewed at low angles. The phase of the ground-reflected component arriving at and returning from the target discriminates against propagation at angles of elevation below the Brewster angle for vertical polarization, and at all low angles for horizontal polarization. The result is that the cross section is usually several orders of magnitude larger for vertical polarization than for horizontal (1, 2, 9, 10). This is the reason for the emphasis on vertical polarization in this report.

X. FIELD MEASUREMENTS BEYOND THE TARGET

While not directly applicable to the measurement of cross sections, measurements of the field at certain points on the side of the target remote from the transmitter are also reported here. The results agree with theoretical expectations.

Field measurements were made along the transmitter-target line and continued beyond the target. Figure 33 shows results for a 16-ft vertical aluminum cylinder standing on the ground (but not grounded with chicken wire). The target chosen was close to a resonant length and therefore scattered a comparatively large amount of energy back toward the transmitter, giving rise to the standing waves described in earlier chapters.

Beyond the target, however, the result was simply a decrease in the field strength at any given range. While this decrease amounted to 50 percent or more close to the target, at ranges greater than about 1.5λ the decrease was about 12 percent.

Measurements of field strength were also performed along a line perpendicular to the transmitter-target line and intersecting with it 60 ft beyond the target. Figure 34 shows some results when Tree I served as the target. A standing wave appears, but now it has a wavelength longer than λ. This is because energy scattered from the side of the target combines with the energy direct from the transmitter in a way that depends on the phase relationship between the two, and this in turn depends on the geometry. If the transmitter can be regarded as infinitely far away, the phase of the direct component is the same all the way along the line of measurement. The phase of the scattered component depends on the number of wavelengths from the tree to the probe, so that far enough from the tree, along the line of measurement, the standing wave has a wavelength equal to λ, but closer in it is larger than λ.

Theoretical calculations by King and Wu [Fig. 3 in Ref. 8] show that at a range of 60 ft beyond the target, the first maximum on either side of the transmitter-target line should be about 73 ft from the line. This agrees well with the maximum on the north side in Fig. 34, but on the south side the maximum is smaller and is at a distance of about

62 ft. This discrepancy can, no doubt, be explained as being due to some asymmetry in the shape of the tree.

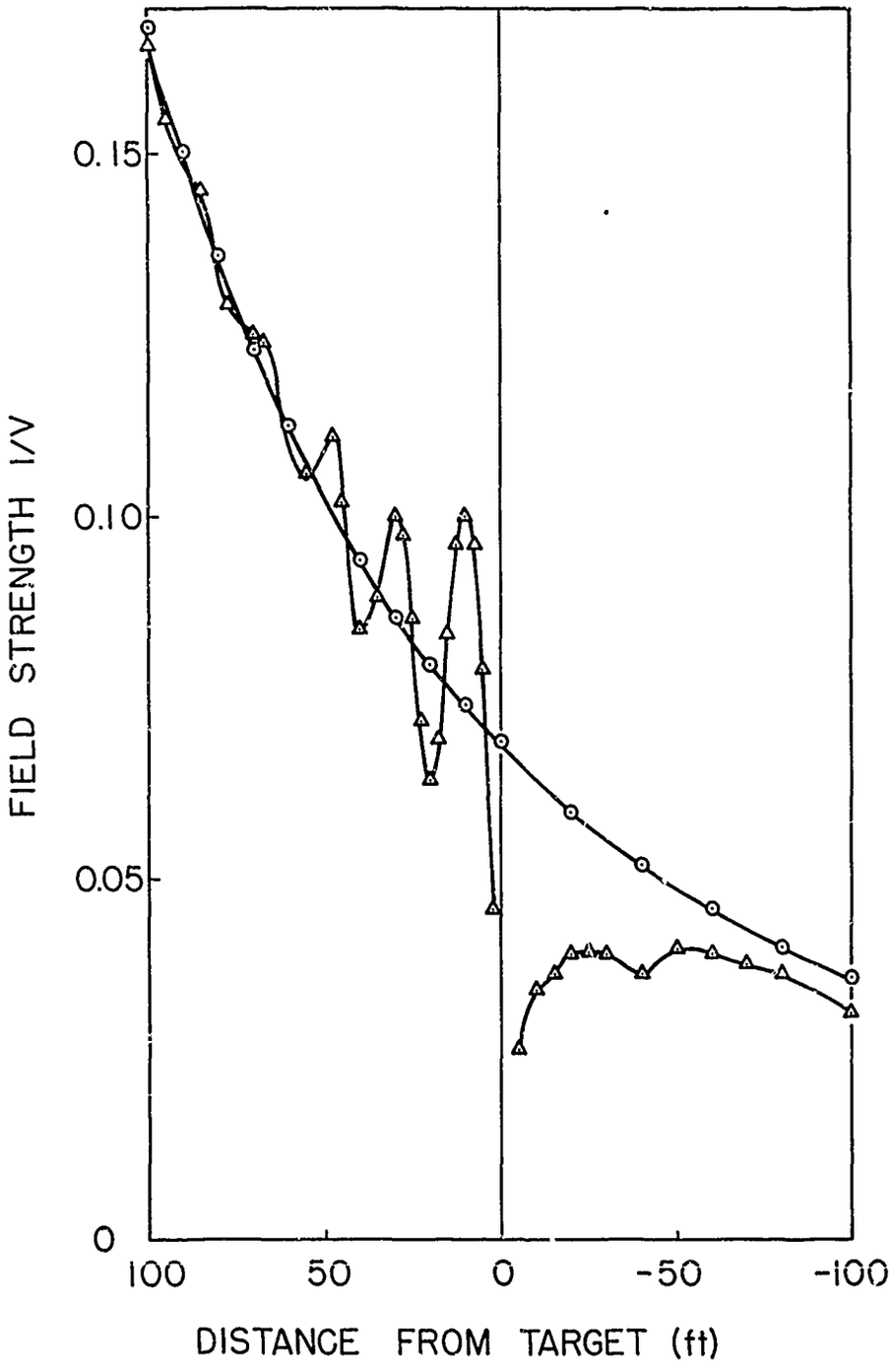

FIG. 33. FIELD STRENGTH ALONG TRANSMITTER-TARGET LINE FOR A 16-FT VERTICAL CYLINDER.

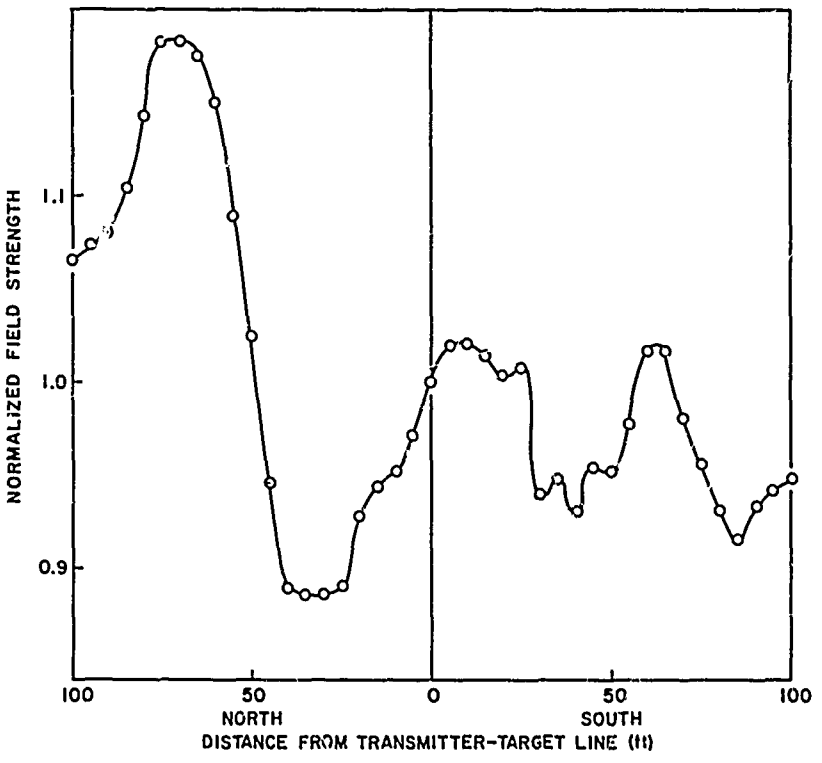

FIG. 34. FIELD STRENGTH ALONG A LINE PERPENDICULAR TO THE TRANSMITTER-TARGET LINE AND 60 FT BEYOND THE TARGET. Tree I was the target.

XI. CONCLUSION

A method of measuring radar cross sections has been developed for use at high frequency.

Measurements of cross sections of oak trees with vertical polarization show that when the main trunk is a quarter of a wavelength long, it behaves like a half-wave dipole. At 25.9 Mc, a half-wave conducting dipole is known to have a cross section of 0.88 λ^2, or 118 m^2. By comparison, a quarter-wave tree was found to have a cross section of 70 m^2, or about 0.6 that of a half-wave dipole.

A tree much smaller than $\lambda/4$ would be expected to have a very much smaller cross section. Therefore, for efficient backscattering at 3 Mc, a tree would need to have a trunk at least 80 ft long, when its cross section would be about 0.88 $\lambda^2 \times 0.6$, or 5280 m^2. At 30 Mc, an 8-ft trunk would suffice, and σ would be about 52.8 m^2.

For vertical polarization, a street light was found to have a cross section of 241 m^2 at 25.9 Mc, while vehicles had cross sections ranging from 0.7 to 28 m^2.

The measuring technique is presently being extended to find the cross section of tree-covered terrain at different angles of elevation and with both horizontal and vertical polarizations; this work will be described in a forthcoming report [Ref. 11]. At this stage, however, it can be noted that a tree is capable of scattering back a considerable amount of energy, and provided its vertical radiation pattern is favorable to the return of energy, a tree should be a major contributor to ground backscatter.

REFERENCES

1. J. G. Steele, "Backscatter of 16 Mc/s Radio Waves from Land and Sea," Austral. J. Phys., 18, 1965, pp. 317-327.

2. J. G. Steele, "Backscatter of Radio Waves from the Ground," Rept. SEL-65-064 (TR No. 109), Stanford Electronics Laboratories, Stanford, Calif., Jun 1965.

3. D. D. King, "The Measurement and Interpretation of Antenna Scattering," Proc. IRE, 37, 1949, pp. 770-777.

4. J. Sevick, "Experimental and Theoretical Results on the Backscattering Cross Sections of Coupled Antennas," Technical Report 150, Cruft Laboratory, Harvard University, Cambridge, Mass., May 1952.

5. B.-O. Ås and H. J. Schmitt, "Backscattering Cross Section of Reactively Loaded Cylindrical Antennas," Scientific Report No. 18, Cruft Laboratory, Harvard University, Cambridge, Mass., Aug 1958.

6. J. H. Van Vleck, F. Bloch, and M. Hamermesh, "Theory of Radar Reflection from Wires or Thin Metallic Strips," J. Appl. Phys., 18, 1947, pp. 274-294.

7. K. Lindroth, "Reflection of Electromagnetic Waves from Thin Metal Strips," Trans. Roy. Inst. Technol., Stockholm, No. 91, 1955.

8. R. W. P. King and T. T. Wu, The Scattering and Diffraction of Waves, Harvard University Press, Cambridge, Mass., 1959.

9. L. B. Wetzel, "On HF Ground Backscatter," Institute for Defense Analyses, Arlington, Va., Oct 1965 (unpublished paper).

10. D. E. Kerr, Propagation of Short Radio Waves, McGraw-Hill Book Company, New York, 1951.

11. J. G. Steele, "High-Frequency Backscatter from Terrain with Trees," Technical Report No. 128, Stanford Electronics Laboratories, Stanford, Calif. (in preparation).

12. J. G. Steele, "Influence of Electrical Properties of the Ground on the Backscatter Coefficient at High Frequency," Rept. SEL-65-110 (TR No. 121), Stanford Electronics Laboratories, Stanford, Calif., Dec 1965.

13. R. P. Basler and T. Scott, "The HF Backscatter Cross Sections of Trees," Electro-Physics Laboratories, ACF Industries Incorporated, Hyattsville, Md., Dec. 1965 (unpublished paper).

UNCLASSIFIED
Security Classification

DOCUMENT CONTROL DATA - R&D

(Security classification of title, body of abstract and indexing annotation must be entered when the overall report is classified)

1. ORIGINATING ACTIVITY (Corporate author)	2a. REPORT SECURITY CLASSIFICATION
Stanford Electronics Laboratories Stanford University Stanford, California	UNCLASSIFIED 2b. GROUP

3. REPORT TITLE

HIGH-FREQUENCY MEASUREMENT OF RADAR CROSS SECTION USING THE STANDING-WAVE METHOD

4. DESCRIPTIVE NOTES (Type of report and inclusive dates)

Technical Report

5. AUTHOR(S) (Last name, first name, initial)

Steele, J. G.
Barnum, J. R.

6. REPORT DATE	7a. TOTAL NO. OF PAGES	7b. NO. OF REFS
March 1966	60	13

8a. CONTRACT OR GRANT NO.	9a. ORIGINATOR'S REPORT NUMBER(S)
Nonr-225(64), NR 088 019 and	Technical Report No. 127
b. PROJECT NO. ARPA Order 196-65	SEL-66-021
c.	9b. OTHER REPORT NO(S) (Any other numbers that may be assigned this report)
d.	

10. AVAILABILITY/LIMITATION NOTICES

11. SUPPLEMENTARY NOTES	12. SPONSORING MILITARY ACTIVITY
	Office of Naval Research and Advanced Research Projects Agency

13. ABSTRACT

The standing-wave method of measuring radar cross sections has been adapted for use at 26 Mc. A target in the middle of a large flat field was illuminated by a transmitter 300 feet away, and a prove was moved along the transmitter-target line to measure the amplitude and position of the standing wave due to the target.

Alluminum dipoles of different lengths were first used as targets, and a correction was applied to the results to take account of any nonuniform illumination of the targets. Both the target cross section and the phase of the scattered radiation varied with the target length in the same way as that predicted from microwave measurements. The results demonstrate the validity of extrapolating microwave measurements to the high-frequency part of the spectrum. Calibration of the system was achieved by using the known cross section of a half-wave dipole.

The technique was used to measure cross sections of trees and other objects, and in some cases the "effective height" of an irregularly shaped tree could be deduced.

DD FORM 1 JAN 64 1473

UNCLASSIFIED
Security Classification

14. KEY WORDS	LINK A		LINK B		LINK C	
	ROLE	WT	ROLE	WT	ROLE	WT
RADAR CROSS SECTION						
HF RADAR						
TREES, RADAR CROSS SECTION						

INSTRUCTIONS

1. ORIGINATING ACTIVITY: Enter the name and address of the contractor, subcontractor, grantee, Department of Defense activity or other organization *(corporate author)* issuing the report.

2a. REPORT SECURITY CLASSIFICATION: Enter the overall security classification of the report. Indicate whether "Restricted Data" is included. Marking is to be in accordance with appropriate security regulations.

2b. GROUP: Automatic downgrading is specified in DoD Directive 5200.10 and Armed Forces Industrial Manual. Enter the group number. Also, when applicable, show that optional markings have been used for Group 3 and Group 4 as authorized.

3. REPORT TITLE: Enter the complete report title in all capital letters. Titles in all cases should be unclassified. If a meaningful title cannot be selected without classification, show title classification in all capitals in parenthesis immediately following the title.

4. DESCRIPTIVE NOTES: If appropriate, enter the type of report, e.g., interim, progress, summary, annual, or final. Give the inclusive dates when a specific reporting period is covered.

5. AUTHOR(S): Enter the name(s) of author(s) as shown on or in the report. Enter last name, first name, middle initial. If military, show rank and branch of service. The name of the principal author is an absolute minimum requirement.

6. REPORT DATE: Enter the date of the report as day, month, year, or month, year. If more than one date appears on the report, use date of publication.

7a. TOTAL NUMBER OF PAGES: The total page count should follow normal pagination procedures, i.e., enter the number of pages containing information.

7b. NUMBER OF REFERENCES: Enter the total number of references cited in the report.

8a. CONTRACT OR GRANT NUMBER: If appropriate, enter the applicable number of the contract or grant under which the report was written.

8b, 8c, & 8d. PROJECT NUMBER: Enter the appropriate military department identification, such as project number, subproject number, system numbers, task number, etc.

9a. ORIGINATOR'S REPORT NUMBER(S): Enter the official report number by which the document will be identified and controlled by the originating activity. This number must be unique to this report.

9b. OTHER REPORT NUMBER(S): If the report has been assigned any other report numbers *(either by the originator or by the sponsor)*, also enter this number(s).

10. AVAILABILITY/LIMITATION NOTICES: Enter any limitations on further dissemination of the report, other than those imposed by security classification, using standard statements such as:

(1) "Qualified requesters may obtain copies of this report from DDC."

(2) "Foreign announcement and dissemination of this report by DDC is not authorized."

(3) "U. S. Government agencies may obtain copies of this report directly from DDC. Other qualified DDC users shall request through _____."

(4) "U. S. military agencies may obtain copies of this report directly from DDC. Other qualified users shall request through _____."

(5) "All distribution of this report is controlled. Qualified DDC users shall request through _____."

If the report has been furnished to the Office of Technical Services, Department of Commerce, for sale to the public, indicate this fact and enter the price, if known.

11. SUPPLEMENTARY NOTES: Use for additional explanatory notes.

12. SPONSORING MILITARY ACTIVITY: Enter the name of the departmental project office or laboratory sponsoring *(paying for)* the research and development. Include address.

13. ABSTRACT: Enter an abstract giving a brief and factual summary of the document indicative of the report, even though it may also appear elsewhere in the body of the technical report. If additional space is required, a continuation sheet shall be attached.

It is highly desirable that the abstract of classified reports be unclassified. Each paragraph of the abstract shall end with an indication of the military security classification of the information in the paragraph, represented as *(TS), (S), (C), or (U)*.

There is no limitation on the length of the abstract. However, the suggested length is from 150 to 225 words.

14 KEY WORDS: Key words are technical meaningful terms or short phrases that characterize a report and may be used as index entries for cataloging the report. Key words must be selected so that no security classification is required. Identifiers, such as equipment model designation, trade name, military project code name, geographic location, may be used as key words but will be followed by an indication of technical context. The assignment of links, rules, and weights is optional.

GPO 886-551